Development/Plasticity/Repair

cAMP Response Element-Binding Protein Regulates Differentiation and Survival of Newborn Neurons in the Olfactory Bulb

Claudio Giachino,[1] Silvia De Marchis,[1] Costanza Giampietro,[1] Rosanna Parlato,[2] Isabelle Perroteau,[1] Günther Schütz,[2] Aldo Fasolo,[1,3] and Paolo Peretto[1]

[1]Department of Animal and Human Biology, University of Turin, 10123 Turin, Italy, [2]German Cancer Research Center, D-69120 Heidelberg, Germany, and [3]Rita Levi Montalcini Center for Brain Repair, University of Turin, 10125 Turin, Italy

The transcription factor cAMP response element-binding protein (CREB) is involved in multiple aspects of neuronal development and plasticity. Here, we demonstrate that CREB regulates specific phases of adult neurogenesis in the subventricular zone/olfactory bulb (SVZ/OB) system. Combining immunohistochemistry with bromodeoxyuridine treatments, cell tracer injections, cell transplants, and quantitative analyses, we show that although CREB is expressed by the SVZ neuroblasts throughout the neurogenic process, its phosphorylation is transient and parallels neuronal differentiation, increasing during the late phase of tangential migration and decreasing after dendrite elongation and spine formation. *In vitro*, inhibition of CREB function impairs morphological differentiation of SVZ-derived neuroblasts. Transgenic mice lacking CREB, in a null CREM genetic background, show reduced survival of newborn neurons in the OB. This finding is further supported by peripheral afferent denervation experiments resulting in downregulation of CREB phosphorylation in neuroblasts, the survival of which appears heavily impaired. Together, these findings provide evidence that CREB regulates differentiation and survival of newborn neurons in the OB.

Key words: **subventricular zone; adult neurogenesis; cell differentiation; radial migration; cell survival; olfactory deafferentation**

Introduction

In the dentate gyrus of the hippocampus and in the subventricular zone (SVZ) of the lateral ventricles, new neurons are generated throughout life in mammals (Altman and Das, 1965; Altman, 1969; Cameron et al., 1993; Luskin, 1993; Lois and Alvarez-Buylla, 1994). The olfactory bulb (OB) of adult mammals is the target of neuroblasts migrating from the SVZ (Luskin, 1993; Lois and Alvarez-Buylla, 1994). Newborn cells in the SVZ migrate tangentially in chains toward the OB. Once in the OB, they leave the SVZ moving radially as single cells and differentiate into interneurons in the granular layer (GrL) and glomerular layer (GL) (Luskin, 1993; Lois and Alvarez-Buylla, 1994; Peretto et al., 1999).

Although much progress has been made in the characterization of stimuli regulating adult neurogenesis in the SVZ/OB system (Alvarez-Buylla and Garcia-Verdugo, 2002; Petreanu and Alvarez-Buylla, 2002; Rochefort et al., 2002; Shingo et al., 2003; Saghatelyan et al., 2004), little is known about intracellular signals influencing this process. cAMP response element-binding protein (CREB) and other transcription factors of the CREB family, such as CREM and ATF1, are potential candidates. CREB is an inducible transcription factor that leads to intracellular changes in response to diverse stimuli (Lonze and Ginty, 2002). CREB-mediated transcription requires its phosphorylation on Ser133 induced by various extracellular signals (Lonze and Ginty, 2002). CREB-mediated gene expression is necessary for survival of multiple neuronal subtypes (Bonni et al., 1999; Riccio et al., 1999; Walton et al., 1999; Monti et al., 2002; Shalizi et al., 2003), and it is involved in differentiation, synaptic plasticity, and memory (Lonze and Ginty, 2002). The involvement of CREB in adult neurogenesis is suggested by studies that demonstrate that newly generated neurons in the hippocampal dentate gyrus are immunoreactive for the Ser133-phosphorylated form of CREB (pCREB) (Bender et al., 2001; Nakagawa et al., 2002b). Moreover, pharmacological treatments that activate the cAMP–pCREB transcription pathway increase proliferation, differentiation, and survival in the adult hippocampus (Nakagawa et al., 2002a,b; Fujioka et al., 2004), whereas cell proliferation and differentiation are reduced in inducible dominant-negative CREB mutants (Nakagawa et al., 2002a; Fujioka et al., 2004).

In the present study, we analyzed the role of CREB within the context of adult neurogenesis in the mouse SVZ/OB system. By using a combination of multiple approaches, we found that although CREB is expressed by the SVZ-derived neuroblasts throughout the neurogenic process, its activation through phos-

Received Jan. 20, 2005; revised,; accepted Sept. 9, 2005.

This work was supported by grants from the Compagnia di San Paolo and Fondo per gli Investimenti della Ricerca di Base (FIRB, RBNE01WY7P). We are grateful to Prof. F. Rossi for providing b-actin-EGFP transgenic mice, advice in cell transplant technique, and useful comments on this manuscript. We thank Dr. C. Vinson for kindly providing the A-CREB expression plasmid and M. Westphal for excellent technical assistance.

Correspondence should be addressed to Dr. Paolo Peretto, Department of Animal and Human Biology, University of Turin, Via Accademia Albertina 13, 10123 Turin, Italy. E-mail: paolo.peretto@unito.it.

DOI:10.1523/JNEUROSCI.3512-05.2005

 0270-6474/05/2510105-14$15.00/0

phorylation correlates with defined stages of neuronal differentiation. *In vitro*, inhibition of CREB reduces the morphological maturation of SVZ-derived neuroblasts. *In vivo*, experimentally induced loss of functional connections from the periphery to the OB results in downregulation of CREB phosphorylation in neuroblasts, which is accompanied by reduced radial migration and survival. Loss of CREB in transgenic mice alters the survival of newly generated neurons in the OB. Our results suggest a novel mechanism by which adult neurogenesis in the OB is regulated by CREB, which supports maturation and survival of SVZ neuronal precursors.

Materials and Methods

Animals and bromodeoxyuridine treatments. Experimental procedures were in accordance with the institutional guidelines for animal welfare. A bromodeoxyuridine (BrdU) time course study and zinc sulfate intranasal irrigation experiments were performed on young adult male mice (2 months old) of CD1 strain (Charles River, Calco, Italy). Generation of $CREB1^{Camkcre4}$ and $CREB1^{Camkcre4}CREM^{-/-}$ mutant mice was described previously (Mantamadiotis et al., 2002). Mice were maintained four to five per cage in rooms with a lighting schedule of 12 h light/darkness and with standard diet and water *ad libitum*. To identify newly generated cells at different survival times, mice were given intraperitoneal injections of BrdU (50 mg/kg body weight in 0.1 M Tris, pH 7.4). For the time course study, young adult CD1 mice underwent two subsequent (every 6 h) BrdU administrations and were killed 2 h, 10 d, 15 d, or 45 d after BrdU administration ($n = 4$ for each time point). For the zinc sulfate intranasal irrigation study (see below), four to five animals for survival time (10, 15, or 45 d) for each treatment (saline or zinc sulfate) were given injections of BrdU twice. To exclude the possibility that zinc sulfate treatment interfered with proliferation of labeled cells, BrdU was injected the day before intranasal irrigation. To identify newly generated cells in mutant mice, 3-month-old $CREB1^{Camkcre4}$ ($n = 3$), $CREB1^{Camkcre4}CREM^{-/-}$ ($n = 5$), and control ($n = 5$) mice received BrdU injections (three per day for 2 d) and were killed 30 d later. Additional $CREB1^{Camkcre4}$, $CREB1^{Camkcre4}CREM^{-/-}$, $CREM^{-/-}$, and control mice were killed at 3, 4, 5, or 7 months of postnatal life for histological analyses ($n = 2$–4 for genotype for each age).

The mice were deeply anesthetized with an intraperitoneal injection of a solution of ketamine (80 μl; Ketavet; Gellini, Aprilia LT, Italy) and xylazine (20 μl; Rompun; Bayer, Wuppertal, Germany). All of the animals were perfused transcardially with 0.9% saline, followed by 4% paraformaldehyde in 0.1 M phosphate buffer, pH 7.4. The brains were postfixed for 6 h in the same solution, cryoprotected in a 30% sucrose solution in 0.1 M phosphate buffer, pH 7.4, frozen, and cryostat sectioned. Free-floating coronal sections (25 μm) were collected in multiwell dishes in series representatives of the SVZ and OB. Sections were stored at −20°C in antifreeze solution until use.

Zinc sulfate intranasal irrigation. Young adult CD1 mice received intranasal administration of zinc sulfate (0.17 M; Sigma, St. Louis, MO) or saline using a method similar to that described by McBride et al. (2003). The mouse was placed in a conical holder that exposed the snout, and the right naris was injected with 100 μl of zinc sulfate or saline. The left naris was injected 10 min later. The solutions were injected by a syringe with a blunted 4-mm-long needle inserted into the naris. After intranasal irrigation, the mouse was held for several seconds with its head down to minimize spread of the solution to the oral cavity. Mice (saline, $n = 12$; zinc sulfate, $n = 21$) were deeply anesthetized and perfused intracardially 9, 14, or 44 d after irrigation.

Stereotaxic surgery and tracer injection. Stereotaxic injections were performed on 2-month-old adult CD1 strain mice (Charles River) as described previously (De Marchis et al., 2001). Briefly, animals were anesthetized by intraperitoneal injection of a 4:1 ketamine:xylazine solution (30–35 μl) and positioned in a stereotaxic apparatus (David Kopf Instruments, Tujunga, CA). Approximately 300–400 nl of Cell Tracker Green CMFDA (CTG; 10 mM dimetheylsulfoxide; Invitrogen, Eugene, OR) was injected at stereotaxic coordinates of 1 mm anterior to bregma, 1 mm lateral to the sagittal sinus, and a 2 mm depth by means of a glass micropipette and a pneumatic pressure injection apparatus (WPI-PV-800; World Precision Instruments, Sarasota, FL). After surgery, the animals were left on a warm platform and monitored constantly until recovery. Mice were deeply anesthetized and perfused intracardially 7 d ($n = 3$) after the tracer injection.

Preparation of cell suspension and transplantation. Donor cells were obtained from transgenic mice overexpressing the enhanced green fluorescent protein (EGFP) under the control of the β-actin promoter produced originally by Okabe et al. (1997) and kindly provided by Prof. F. Rossi (University of Turin, Turin, Italy) (Carletti et al., 2002). Postnatal day 1 (P1) to P2 mice were deeply anesthetized by hypothermia and decapitated rapidly, and the brain was dissected out in PBS with 0.6% glucose (PBG). Forebrains harvested from 10 mice were embedded in a solution of 3% low-gelling agarose (Sigma) in L-15 medium (Invitrogen, Gaithersburg, MD) and vibratome cut into 300-μm-thick coronal slices collected in L-15 medium. Under a high-magnification dissecting microscope, the SVZ of the lateral ventricle was carefully dissected away from surrounding brain structures, isolated, and mechanically dissociated to a single-cell suspension by means of a P200 Gilson pipette. The cell suspension was then centrifuged ($1000 \times g$ for 7 min) and resuspended in 40 μl of PBG.

Cell transplantation was performed on 2-month-old CD1 mice (Charles River), following the same surgical procedure described before for neuronal tracer injection. One to 2 μl of EGFP cell suspension was injected at stereotaxic coordinates of 1 mm anterior to bregma, 1 mm lateral to the sagittal sinus, and a depth of 2 mm. The mice were deeply anesthetized and perfused intracardially 15 d ($n = 4$) or 1 month ($n = 5$) after surgery.

Plasmid construction. DNA manipulations were performed using standard techniques (Sambrook et al., 1999). A CMV500–4hep-CREBLZ(MO) plasmid, containing the coding sequence for a mutant form of CREB (A-CREB), which acts as a dominant repressor of wild-type CREB by the formation of a nonbinding heterodimer, was kindly provided by Dr. C. Vinson (National Cancer Institute, Bethesda, MD) (Ahn et al., 1998). A plasmid-expressing fusion protein was constructed by an in-frame insertion of the coding sequence of A-CREB mutant into the *Bam*HI gap of pEGFP-C3 vector (Clontech, Palo Alto, CA). pEGFP-C3-A-CREB expression vectors were identified by the *Hind*III restriction map.

Primary cultures, inhibitors, and transient transfections. Primary cell cultures were prepared from P4–P8 CD1 mice. The SVZ/OB was dissected carefully (see above), trypsinized for 5 min at 37°C (trypsin; Invitrogen, San Diego, CA), and mechanically dissociated. The obtained cell suspension was centrifuged and resuspended in serum-free Neurobasal medium enriched with 1× B27 supplement (Invitrogen, Gaithersburg, MD), 25 μg/ml gentamicin (Seromed, Berlin, Germany), and 0.5 mM glutamine (Sigma), and cells were seeded at the density of 2.2×10^4 cells/cm^2 (experiments with inhibitors) or 3.5×10^4 cells/cm^2 (transfections) onto sterile coverslips previously coated with poly-D-lysine (Sigma). Cultures were kept at 37°C in a humidified atmosphere containing 5% CO_2. Inhibition of CREB activity was performed by pharmacological treatments with kinases inhibitors or by transfection of the dominant-negative pEGFP-C3-A-CREB expression vector. SVZ primary cultures were treated for 48 h, starting from 2 h after seeding, with vehicle (DMSO) as a control or with one of the following inhibitors: calcium/calmodulin (CaM) kinase inhibitor KN62 (10 mM; Calbiochem, La Jolla, CA), phosphatidylinositol 3-kinase (PI3 kinase) inhibitor 2-(4-morpholinyl)-8-phenyl-4*H*-1-benzopyran-4-one (LY294002; 5 mM; Sigma), mitogen-activated protein (MAP) kinase inhibitor 2′-amino-3′-methoxy flavone PD98059 (10 mM; Calbiochem), or cAMP-dependent kinase inhibitor Rp-cAMP (*R*p isomer of adenosine-3′,5′-cyclic monophosphorothioate) (10 mM; BioLog, Hayward, CA). Cells were fixed with 4% paraformaldehyde (PFA) at 2 d *in vitro* (DIV) and processed for double immunocytochemistry. Transient transfections were performed 2 h after seeding SVZ neuronal precursors by using Lipofectamine 2000 transfection reagent (Invitrogen, San Diego, CA) according to the manufacturer's instructions. For each transfection experiment, 5 μg of the pEGFP-C3-A-CREB expression vector and 2 μl of Lipofectamine 2000 per milliliter of antibiotic-free culture medium were used. Transfection

of pEGFP-C3 empty vector was used as control. After 4 h of incubation, transfection solution was removed, and cells were washed with PBS with Ca^{2+}/Mg^{2+} and incubated for 48 h with culture medium. At 2 DIV, cells were fixed with 4% PFA and immunostained for βIII tubulin and GFP.

Immunohistochemistry. For BrdU immunostaining, sections were treated with 2N HCl for 1 h at 37°C and neutralized with borate buffer, pH 8.5. Sections were incubated for 48 h at 4°C in primary antibody diluted in 0.01 M PBS, pH 7.4, 0.5% Triton X-100, and 1% normal serum. The primary antibodies used were anti-BrdU (1:3000 for the avidin–biotin–peroxidase method, 1:1000 for immunofluorescence; monoclonal rat IgG; Harlan, Zeist, The Netherlands), anti-CREB (1:300; rabbit IgG; Cell Signaling, Beverly, MA), anti-pCREB (1:400; rabbit IgG; Cell Signaling), anti-activated caspase-3 (1:3000; rabbit; CM1 antibody; Idun Pharmaceuticals, La Jolla, CA), anti-polysialylated form of the neural cell adhesion molecule (PSA-NCAM; 1:2500; monoclonal mouse IgM; Ab-Cys, Paris, France), anti-NeuN (neuron-specific nuclear protein; 1:800; monoclonal mouse IgG; Chemicon, Temecula, CA), anti-doublecortin (1:500; goat; C-18 antibody; Santa Cruz Biotechnology, Santa Cruz, CA), anti-GFAP (1:1000; monoclonal mouse IgG; Boheringer, Mannheim, Germany), anti-Cre recombinase (1:1000; rabbit; Covance Research Products, Denver, PA), anti-GFP (1:500; rabbit; Invitrogen), and anti-olfactory marker protein (OMP; 1:10,000; goat; generous gift from Prof. F. L. Margolis, University of Maryland, Baltimore, MD). For the avidin–biotin–peroxidase method, sections were incubated for 1 h at room temperature in secondary biotinylated antibody (anti-rat IgG, anti-rabbit IgG, or anti-goat IGG; Vector Laboratories, Burlingame, CA) diluted 1:250 in 0.01 M PBS, pH 7.4, and 0.5% Triton X-100, followed by the avidin–biotin–peroxidase complex (Vector Laboratories). To reveal immunoreactivity, we used 0.015% 3,3′-diaminobenzidine and 0.0024% H_2O_2 in 0.05 M Tris-HCl, pH 7.6. After adhesion on (3-aminopropil)trietoxysilane-coated slides (Tespa; Sigma), sections were dehydrated and mounted in Sintex (Nuova Chimica, Cinisello Balsamo, Italy). For immunofluorescent double labeling, sections were incubated in a mixture of two primary antibodies and appropriate blocking sera for 48 h at 4°C, followed by appropriate Cy3-conjugated secondary antibody and biotinylated secondary antibody, followed by avidin-FITC. For immunocytochemistry of primary cultures, cells were incubated overnight in primary antibody diluted in 0.01 M PBS, pH 7.4, 1% normal serum, and 0.1% Triton X-100.

For double labeling with BrdU, sections were incubated for 48 h at 4°C in anti-NeuN, anti-pCREB, anti-CREB, or anti-PSA-NCAM primary antibody and appropriate serum and then incubated for 1 h at room temperature in secondary antibody [Cy3 anti-mouse IgG+IgM (Jackson ImmunoResearch, West Grove, PA) or Cy3 anti-rabbit (Sigma)] diluted 1:800. Sections were then treated with 2 M HCl for 30 min at 37°C, neutralized with borate buffer, pH 8.5, and incubated for 24 h at 4°C in primary anti-BrdU antibody and appropriate serum. Sections were incubated for 1 h at room temperature in secondary biotinylated antibody (anti-rat IgG mouse-adsorbed; Vector Laboratories) diluted 1:250, followed by avidin-FITC (Vector Laboratories). Sections were mounted, air dried, and coverslipped in polyvinyl alcohol with diazabicyclo-octane as an anti-fading agent.

Quantification and statistical analyses. Fluorescent signals were detected using an Olympus (Melville, NY) FV 200 Fluoview confocal laser-scanning microscope equipped with a 100× objective. Randomly selected cells were analyzed with fixed photo multiplier settings, to minimize rating variations between sections and animals. Fifty cells per region of interest (30 in the GL) were examined for colabeling in each animal ($n = 4–8$ animals in each group). Data are presented as the average percentage of colabeled cells. In primary cultures of the SVZ, newborn neurons colabeled with βIII tubulin and pCREB or βIII tubulin and GFP were subjected to morphometric analysis. Four dishes from each of three independent experiments were analyzed. Twenty-five neurons in each dish were selected randomly, and the length of dendrites, number of primary dendrites, and number of dendritic branches were determined. The dendritic length was measured by drawing all βIII tubulin-labeled processes with the image analysis software Image Pro-Plus 4.1 for Windows (1994, 1999; Media Cybernetics, Silver Spring, MD). The remaining parameters were scored manually on the image. Processes <5 μm were excluded from the analysis.

To evaluate the rate of cell migration and survival in different experimental groups, coronal sections (one every 300 mm) from the right hemisphere were immunohistochemically labeled for BrdU or active caspase-3 and analyzed. Labeled cells were counted in coronal sections of the anterior SVZ and OB ($n = 4–6$ for each group). Sections were analyzed by means of an image analysis workstation based on an Olympus microscope, a camera (CoolSNAP-Pro color RS Photometrics; Media Cybernetics), and the image analysis software Image Pro-Plus 4.1 for Windows. The area of the SVZ or GrL was measured, and the number of labeled cells within the selected region was determined. BrdU-labeled cells in the GrL were counted within a 100 × 100 mm counting frame positioned with its side at the SVZ/GrL boundary (deep GrL) or at the mitral cell layer/GrL boundary (superficial GrL). The collected data were used to estimate the number of labeled cells per square millimeter. Data are presented as means ± SEM. Statistical comparisons were conducted by Student's *t* test or by one-way ANOVA, followed by the Newman–Keuls (NK) *t* test. Significance was established at $p < 0.05$.

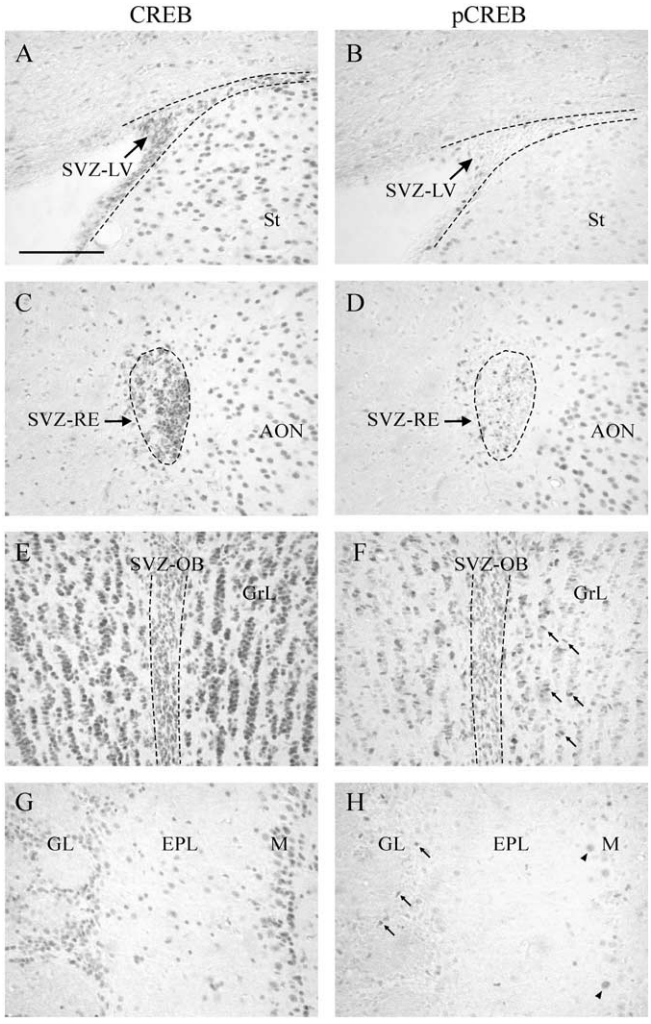

Figure 1. CREB and pCREB expression in the SVZ/OB system. CREB immunoreactivity is found in the majority of cells within the SVZ (dashed lines) and the OB (***A***, ***C***, ***E***, ***G***), whereas pCREB immunoreactivity is found in scattered cells (***B***, ***D***, ***F***, ***H***). ***F***, pCREB-labeled cells are particularly numerous within the anterior SVZ (SVZ-OB) and within the OB GrL (arrows). ***H***, pCREB-positive cells are also found within the GL (arrows) and M layer (arrowheads), whereas they are rare within the EPL. ***A–D***, CREB- and pCREB-positive cells are also visible in the striatum and the accessory olfactory nucleus adjacent to the SVZ. Scale bar, 100 μm. M, Mitral cell layer; St, striatum; AON, anterior olfactory nucleus.

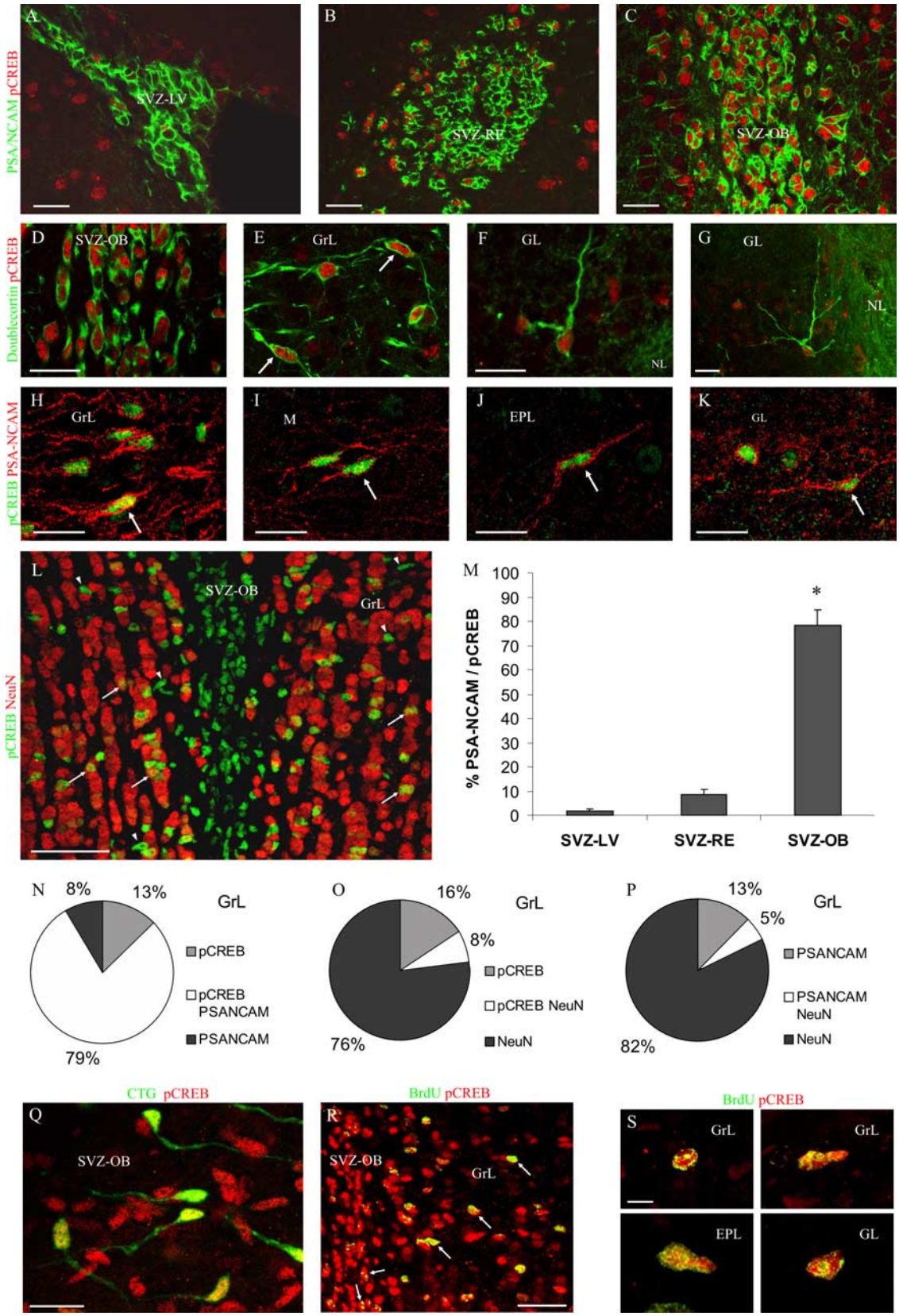

Figure 2. CREB phosphorylation in SVZ-derived newly generated cells. ***A–C***, pCREB-immunoreactive cells within the SVZ are PSA-NCAM positive. Note that pCREB-labeled cells are rare within the SVZ-LV and SVZ-RE, whereas they are numerous within the SVZ-OB. ***D–G***, pCREB-immunoreactive cells within the SVZ (***D***) and OB (***E–G***) layers are doublecortin positive. Some cells, particularly within the GL, show a branched morphology (***G***). ***H–K***, pCREB-immunoreactive cells within the OB are PSA-NCAM positive. Note that many pCREB-positive cells double labeled with doublecortin or PSA-NCAM show a bipolar morphology (arrows; ***E***, ***H–K***). ***L***, Both pCREB+/NeuN− (arrowheads) and pCREB+/NeuN+ (arrows) cells are found within the OB GrL. Many pCREB+/NeuN− cells are located within the anterior SVZ. ***M***, Quantification of PSA-NCAM+/pCREB+ double-immunoreactive cells within the SVZ-LV, SVZ-RE, and SVZ-OB (same levels as in ***A–C***). Data are presented as the percentage of PSA-NCAM+ cells that are also pCREB+. CREB phosphorylation in neuroblasts dramatically increases within the anterior SVZ. *$p < 0.05$, significant (*Figure legend continues.*)

Results

CREB- and pCREB-immunoreactive cells in the SVZ and OB of the adult mouse

The pattern of CREB and pCREB localization was examined by immunohistochemistry in serial coronal sections of the forebrain representative of the entire SVZ, from the SVZ of the lateral ventricle (SVZ-LV) to its rostral extension (SVZ-RE) including its most anterior part in the core of the OB (SVZ-OB).

Most of the cells in the entire SVZ and in the OB showed strong nuclear staining for CREB, demonstrating that this transcription factor is ubiquitous in the SVZ/OB system (Fig. 1*A*,*C*,*E*,*G*). In contrast, immunostaining for pCREB (the active phosphorylated form of CREB) within the SVZ was not uniformly distributed (Fig. 1*B*,*D*,*F*). Interestingly, a posteroanterior gradient of pCREB-positive cells was observed in the SVZ. Only few scattered nuclei were pCREB positive in the SVZ-LV and SVZ-RE (Fig. 1*B*,*D*), whereas the majority of CREB-positive cells in the SVZ-OB were also positive for the phosphorylated form of CREB (Fig. 1*E*,*F*). Within the OB, pCREB immunostaining was not restricted to the SVZ; it was localized also in scattered cells distributed over the OB layers (Fig. 1*F*,*H*). The majority of these cells were located within the GrL and GL, which are the final targets of SVZ migrating neuroblasts, and showed small round, irregular, or elongated pCREB-immunopositive nuclei (Fig. 1*F*,*H*, arrows). A few large, round, labeled nuclei were also found in the mitral cell layer (Fig. 1*H*, arrowheads). Besides the SVZ/OB system, CREB-immunoreactive cells were observed in more posterior brain regions adjacent to the SVZ, such as the striatum (Fig. 1*A*, St) and the accessory olfactory nucleus, where an intense pCREB immunoreactivity was also observed (Fig. 1*C*,*D*). The pCREB staining intensity was variable among cells, suggesting different levels of activation.

CREB phosphorylation in SVZ-derived newly generated cells

To investigate the phenotype of pCREB-labeled cells in the SVZ and OB, we performed double immunolabeling experiments with glial and neuronal markers. We used an anti-GFAP antibody to label astrocytes, anti-PSA-NCAM and anti-doublecortin antibodies to identify SVZ neuroblasts, and an anti-NeuN antibody to label mature neurons. pCREB-positive cells never express GFAP (data not shown). Conversely, the vast majority of pCREB-positive cells in the entire SVZ expressed PSA-NCAM and doublecortin (Fig. 2*A–D*) and showed a bipolar morphology typical of migrating neuroblasts. To further characterize these cells, we stereotaxically injected the CTG dye into the SVZ-LV. CTG injection is a reliable method for labeling migrating SVZ progenitors (De Marchis et al., 2001, 2004). CTG-labeled cells were present along the SVZ/OB system after a 7 d survival. At this time, numerous CTG-positive neuroblasts reached the SVZ in the core of the OB and showed a strong pCREB immunopositivity (Fig. 2*Q*), confirming the migratory nature of these cells. At different levels along the SVZ, we quantified the percentage of PSA-NCAM-positive migrating neuroblasts that is also pCREB immunoreactive and found that it was very low in the SVZ-LV (1.7%) and in the SVZ-RE (8%) but dramatically increased in the SVZ-OB (78%) (ANOVA: $F = 114.69$, $p < 0.001$; NK t test, $p < 0.05$; SVZ-LV vs SVZ-OB and SVZ-RE vs SVZ-OB) (Fig. 2*A–C*,*M*), indicating that strong CREB activation occurs in the SVZ cells during the last part of their tangential migration. Numerous double-labeled pCREB/PSA-NCAM and/or doublecortin cells with a bipolar morphology (Fig. 2*E*,*H–K*, arrows) were also found in the OB layers, where only a few double-labeled cells showed a branched morphology (Fig. 2*G*). Interestingly, pCREB immunoreactivity was also observed associated to NeuN-positive mature neurons in the GrL (Fig. 2*L*, arrows) and GL (data not shown) of the OB. To evaluate the relative degree of expression of pCREB in neuronal elements at different maturation stages in the OB, we quantified the percentage of pCREB and PSA-NCAM or NeuN double-labeled cells in the GrL. We found high levels of pCREB/PSA-NCAM coexpression and low percentages of pCREB/NeuN double-labeled cells (Fig. 2*N*,*O*). It is noteworthy that a certain degree of colocalization was observed between PSA-NCAM and NeuN (Fig. 2*P*). These data indicate that both within the SVZ and the OB-GrL, the majority of pCREB-positive cells are neuroblasts.

CREB is transiently phosphorylated in newly generated cells

Adult neurogenesis is typically detected by incorporation of the exogenous proliferation marker BrdU into dividing cells. Killing animals at different survival times after BrdU administration allows the study of proliferation, migration, and survival of labeled cells in the SVZ/OB system (Petreanu and Alvarez-Buylla, 2002; Winner et al., 2002; Brown et al., 2003).

In this study, survival times of 2 h, 10 d, 15 d, and 45 d after BrdU injection were selected to identify, respectively, proliferating cells in the SVZ (2 h), cells migrating tangentially in the SVZ and radially in the OB (10 d), differentiating cells (15 d), and fully mature newly generated cells (45 d) in the OB GrL and GL. At the earliest survival time analyzed (2 h), we did not observe any colabeling of pCREB and BrdU in the SVZ, indicating that CREB is not phosphorylated in proliferating cells (Fig. 3*A*). At 10 d survival, BrdU-positive cells migrated anteriorly, and the majority of them (69.5%) were pCREB immunoreactive in the rostral portion of the SVZ within the OB (Figs. 2*R*, 3*A*). This result indicates that massive CREB phosphorylation occurs during the last part of tangential migration (t test; $p < 0.001$; SVZ-LV vs SVZ-OB). At this survival time, high percentages of BrdU-positive cells expressing pCREB were also found both in the OB GrL (73.5%) and GL (61.7%) (Figs. 2*R*,*S*, 3*B*,*C*). Fifteen days after BrdU injection, these percentages significantly decreased to values of 43.5 and 35.8%, respectively, in the OB GrL and GL (Fig. 3*B*,*C*). Forty-five days after injection, the percentage of double-labeled cells was further reduced to 7% in the GrL and 4.2% in the GL, suggesting that CREB phosphorylation is downregulated in fully mature cells (GrL: ANOVA, $F = 159.71$, $p < 0.001$; NK t test, $p < 0.05$; 10 vs 15 and 15 vs 45 d; GL: ANOVA, $F = 63.17$, $p < 0.001$; NK t test, $p < 0.05$; 10 vs 15 and 15 vs 45 d) (Fig. 3*B*,*C*). These data are consistent with a transient activation of CREB in newly generated cells and indicate that the time window in which CREB is phosphorylated includes the last part of the tangential migration

←

(*Figure legend continued.*) difference from SVZ-LV and SVZ-RE. ***N–P***, Coexpression of pCREB, PSA-NCAM, and NeuN within the OB GrL. PSA-NCAM and pCREB expression primarily overlap (***N***). In contrast, a low degree of coexpression was found between both pCREB and NeuN (***O***) and PSA-MCAM and NeuN (***P***). ***Q***, CTG-labeled cells, showing the typical morphology of migrating neuroblasts, are pCREB immunoreactive in a parasagittal section of the SVZ-OB. ***R***, ***S***, Ten days after BrdU injection, many BrdU+/pCREB+ cells are found within the anterior SVZ and the OB layers (arrows). Note that many double-labeled cells show elongated nuclei, suggesting that they are still migrating. M, Mitral cell layer; NL, olfactory nerve layer. Error bars indicate SEM. Scale bars: ***A–K***, ***Q***, 20 μm; ***L***, ***R***, 50 μm; ***S***, 5 μm.

within the SVZ of the OB, the radial migration through OB layers, and possibly differentiation.

CREB phosphorylation parallels cell differentiation

It has been shown previously that during differentiation, newly generated cells in the OB downregulate PSA-NCAM and doublecortin and upregulate NeuN (Petreanu and Alvarez-Buylla, 2002; Winner et al., 2002; Brown et al., 2003; Petridis et al., 2004). Our findings indicated colocalization of pCREB and doublecortin in cells with a branched morphology, as well as the occurrence of pCREB/NeuN double-labeled cells, in the OB (Fig. 2*G*,*L*). However, our BrdU birth-dating study showed a progressive dephosphorylation of CREB in cells at 15 and 45 d after injection. By correlating the number of double-labeled pCREB/BrdU cells with that of double-stained PSA-NCAM/BrdU and NeuN/BrdU neuronal elements in the OB, it became evident that the percentages of pCREB+/BrdU+ and PSA-NCAM+/BrdU+ elements followed the same trend progressively decreasing with the time, whereas NeuN+/BrdU+ cells (Fig. 4) showed the opposite trend. Interestingly, NeuN expression in BrdU-positive cells was sharply increased (up to 88.5%) in the GrL at a 15 d survival time when 43.5% of BrdU-labeled cells were still positive for pCREB (Fig. 4). At 45 d after injection, most of BrdU-positive cells in the GrL were NeuN positive and pCREB negative. These results, together with the observation that a certain degree of colocalization occurred between PSA-NCAM and NeuN (Fig. 2*P*), indicate that CREB phosphorylation lasts in newly generated cells during neuronal differentiation when cells shift from PSA-NCAM expression to NeuN expression.

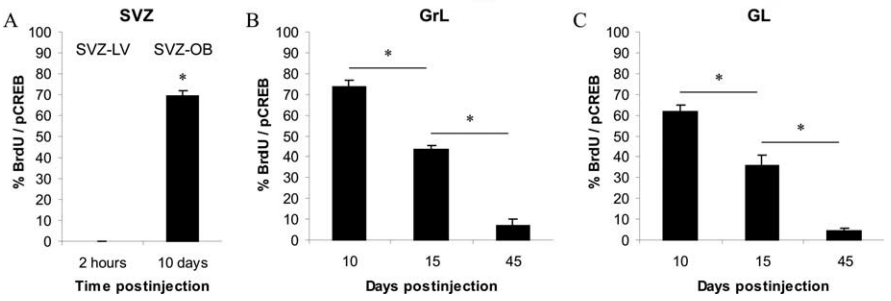

Figure 3. Time course of BrdU+/pCREB+ double-immunoreactive cells within the SVZ and OB. Data are presented as the percentage of BrdU+ cells that are also pCREB+. ***A***, CREB phosphorylation is undetected in proliferating cells within the SVZ-LV, whereas it increases in tangentially migrating cells toward the OB (see also Fig. 2 *A–C*, *M*). ***B***, ***C***, After newly generated cells attain their final position within the OB GrL and GL, CREB phosphorylation is downregulated. The asterisk indicates a significant difference. Error bars indicate SEM.

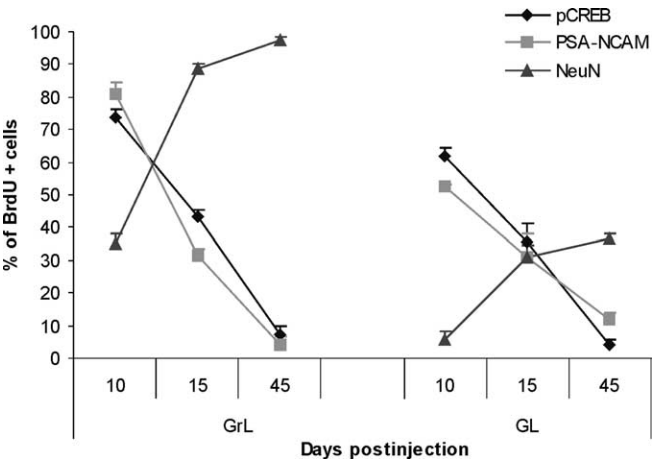

Figure 4. Time course of pCREB, PSA-NCAM, and NeuN expression in BrdU-labeled cells within sites of terminal differentiation in the OB. Data are presented as the percentage of BrdU+ cells that express pCREB, PSA-NCAM, or NeuN at each time point within the OB granular and glomerular layers. pCREB downregulation parallels PSA-NCAM downregulation in differentiating newly generated cells. Note that NeuN upregulation initiates before pCREB is downregulated. Error bars indicate SEM.

Colabeling of BrdU with NeuN is useful to identify mature newly generated cells but does not allow identification of their maturation stage. Indeed, maturing newly generated cells of the OB GrL opportunely marked in their processes can be classified in different morphological classes as described previously (Petreanu and Alvarez-Buylla, 2002). In this study, we adopted a cell transplant approach, using EGFP transgenic mice as donors, to efficiently visualize the morphology of newly generated cells as they migrate to and integrate into the OB. After homotopic engraftment of SVZ-derived cells, transplanted neuroblasts appropriately migrate within the SVZ and integrate into the OB (Jankovski and Sotelo, 1996). We analyzed CREB phosphorylation in EGFP-positive cells in the OB 15 d and 1 month after grafting (Fig. 5). According to previous studies (Petreanu and Alvarez-Buylla, 2002; Carleton et al., 2003), EGFP-positive cells in the SVZ and OB GrL were classified as follows: class 1, corresponding to tangentially migrating neuroblasts in the SVZ of the OB (Fig. 5*A*); class 2, represented by radially migrating neuroblasts in the GrL (Fig. 5*B*); class 3, maturing granule neurons with a growing apical dendrite in the GrL that does not cross the mitral cell layer (Fig. 5*C*); class 4, granule cells with branched apical dendrites reaching the external plexiform layer (EPL) but few or no spines (Fig. 5*D*); and class 5, composed of granule cells with many spines on the branched apical dendrites (Fig. 5*E*,*F*). We also introduced three new morphological classes for SVZ neuroblasts located in the EPL and in the GL (Fig. 5*G–I*): class 6, represented by bipolar neuroblasts in the EPL with a simple morphology reminiscent of migrating cells (Fig. 5*G*); class 7, cells in the GL with an elongated cell body and few ramified processes (Fig. 5*H*); and class 8, cells in the GL with a round cell body and multiple branched dendrites (Fig. 5*I*). EGFP-positive cells belonging to all of the described classes were observed in the OB 15 d after transplants (Fig. 5). At this time, CREB phosphorylation was observed in the majority of EGFP-positive cells (Fig. 5*J*,*K*). The percentage of pCREB-labeled cells was not significantly different between classes (ANOVA; class 1–5 cells: $F = 1.93$, $p = 0.158$; class 6–8 cells: $F = 2.33$, $p = 0.153$) (Fig. 5*J*,*K*). One month after grafting, the vast majority of EGFP-positive cells attained a mature morphology (classes 5 and 8), and the percentage of double-labeled EGFP/pCREB cells dramatically decreased (*t* test; 15 d vs 1 month: class 5, $p < 0.01$; class 8, $p < 0.001$) (Fig. 5*J*,*K*). These results demonstrate that CREB activation in newly generated cells persists after the cells reach the OB during the entire process of maturation and indicate that CREB becomes dephosphorylated after attainment of a fully mature morphology.

Inhibition of CREB function impairs the morphological differentiation of SVZ-derived neuroblasts in primary cultures

To investigate a putative role of CREB in cell differentiation, we interfered with CREB function in primary cultures of SVZ neuronal precursors. Cells were harvested by microdissecting the ante-

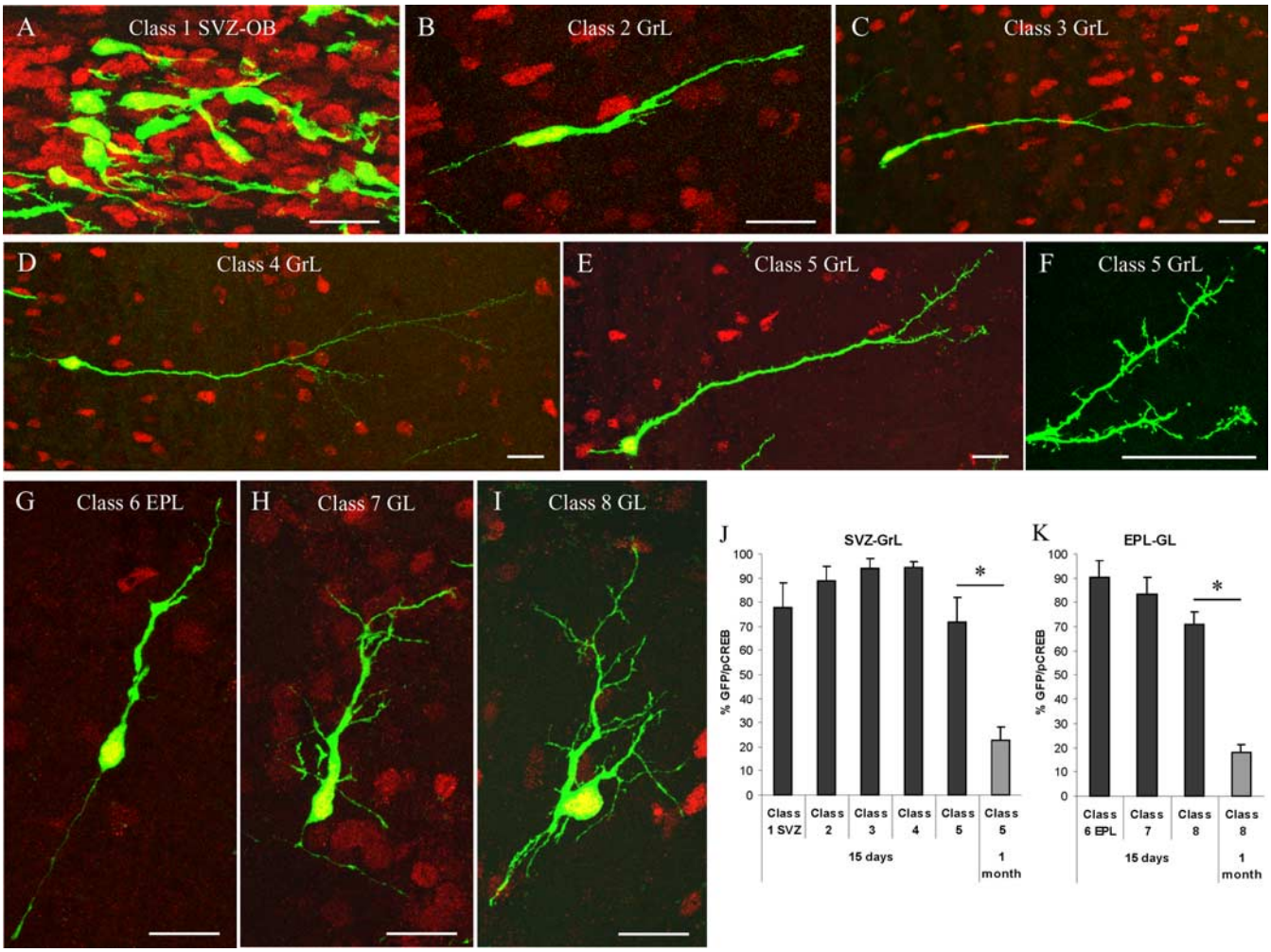

Figure 5. CREB phosphorylation parallels cell differentiation. ***A–I***, GFP-positive cells (green) are pCREB immunoreactive (red) 15 d after transplantation. ***A–F***, Representative images of different morphological maturation stages in the OB SVZ GrL 15 d after transplants of GFP-positive SVZ cells (see Results). Note the presence of synaptic spines on class 5 cell apical dendrites (***F***). ***G–I***, Representative images of different morphological maturation stages in the OB EPL-GL 15 d after transplants of GFP-positive SVZ cells. ***J***, ***K***, Quantification of GFP+/pCREB+ double-positive cells within the SVZ-OB/GrL (***J***) and EPL-GL (***K***) 15 d and 1 month after transplants of GFP-positive cells. Data are presented as the percentage of GFP+ cells. At 15 d, pCREB immunoreactivity is observed in the majority of newborn cells belonging to all of the different maturation classes. One month after grafting, the vast majority of GFP-positive cells attain a mature morphology (class 5, class 8). At this time point, only ~20% of GFP-positive class 5 and class 8 cells are pCREB immunoreactive. Error bars indicate SEM. Scale bars, 20 μm.

rior SVZ (SVZ-OB) from P4–P8 mice and cultured *in vitro* up to 7 d. SVZ-derived cells in culture survived and developed as neurons under serum-free conditions, as observed previously in other studies (Gascon et al., 2005). By double immunocytochemistry for CREB and the neuronal marker βIII tubulin, we showed that all SVZ-cultured neurons express CREB protein (Fig. 6*A*). To determine the time course of CREB phosphorylation in SVZ neuroblasts *in vitro*, we examined the expression of pCREB from 1 to 7 d after plating. In agreement with previous results (Gascon et al., 2005), on day 1, most of the SVZ-derived cells had a round shape with no or few processes (Fig. 6*B*). At this stage, pCREB immunoreactivity was observed in 49% of βIII tubulin-positive cells. The percentage of β-tubulin/pCREB colabeled cells, in parallel with the extension of dendritic processes, increased by day 2 and remained high at day 4 (2 DIV, 85%; 4 DIV, 81%; ANOVA: $F = 6.85$, $p < 0.01$; NK t test, $p < 0.05$; 1 vs 2 and 4 DIV) (Fig. 6*C*,*D*,*F*). One week after plating, CREB phosphorylation was still observed in the majority of cultured newborn neurons (76%) (Fig. 6*E*,*F*), albeit staining intensity was reduced. These results indicate that CREB phosphorylation is strongly induced during the differentiation of the SVZ-derived neurons *in vitro*, supporting our *in vivo* observations.

To interfere with CREB activation, SVZ primary cultures were incubated with inhibitors of different protein kinases involved in CREB phosphorylation (Lonze and Ginty, 2002) in the context of neuronal differentiation (Redmond et al., 2002; Rodgers and Theibert, 2002; Canon et al., 2004; Fujioka et al., 2004), namely CaM kinases, PI3 kinase, MAP kinases, and cAMP-dependent protein kinases. Cells were treated with either each inhibitor or vehicle as a control for 48 h, starting from 0 DIV. Cells were then immunostained with anti βIII tubulin and anti-pCREB antibodies, and the percentage of pCREB-positive neuroblasts was quantified. Incubation with inhibitors of either CaM kinases (Fig. 6*G*, KN62) or PI3 kinase (Fig. 6*H*, LY294002) significantly reduced the number of pCREB-positive neuroblasts (Fig. 6*K*) impairing the strong increase in pCREB observed in controls by 2 DIV (Fig. 6*F*). In contrast, inhibitors of either MAP kinases (Fig. 6*I*, PD98059) or cAMP-dependent protein kinases (Fig. 6*J*, Rp-cAMP) had no effects on CREB phosphorylation (Fig. 6*K*) (ANOVA: $F = 13.24$, $p < 0.001$; NK t test, $p < 0.05$; KN62 and

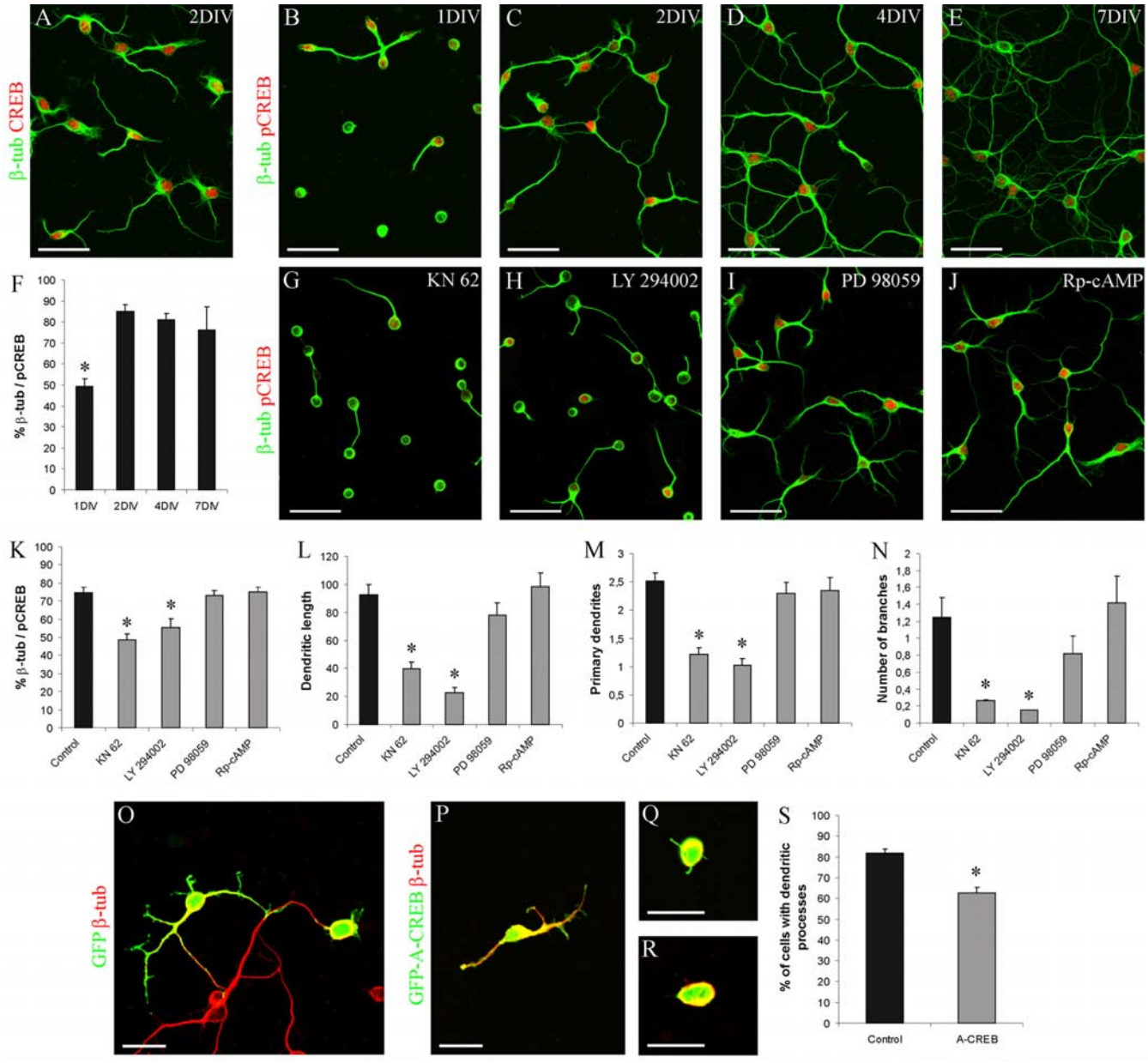

Figure 6. Inhibition of CREB reduces differentiation of SVZ neuroblasts *in vitro*. ***A***, All β-tubulin-positive cells express CREB. Time course of β-tubulin/pCREB colabeled cells. ***B–F***, CREB phosphorylation is significantly upregulated during differentiation by 2 DIV (***F***). ***G–N***, CaM and PI3 kinase inhibitors KN62 (***G***) and LY294002 (***H***) significantly reduce CREB phosphorylation (***K***) and dendritic growth (***L–N***) of β-tubulin-positive cells at 2 DIV, whereas the MAP kinase inhibitor PD98059 (***I***) and the cAMP antagonist Rp-cAMP (***J***) have no effects on either CREB phosphorylation (***K***) or morphological differentiation (***L–N***). Transfection with a dominant-negative form of CREB (***P–R***) significantly reduces the percentage of β-tubulin neuroblasts, which extend dendritic processes, compared with control (***O***). The asterisk indicates a significant difference from the following: 2–7 DIV (***F***); control, PD98059, and Rp-cAMP (***K–M***); control and Rp-cAMP (***N***); control (***S***). Error bars indicate SEM. Scale bars: ***A–E***, ***G–J***, 40 μm; ***O–R***, 20 μm. β-tub, β-Tubulin.

LY294002 vs vehicle, PD98059, and Rp-cAMP). These data indicate that CaM kinases an PI3 kinase are involved in CREB phosphorylation in the SVZ/OB system. We then analyzed whether treatments reducing CREB phosphorylation affected also the morphological differentiation of SVZ precursors. Morphometric analysis of βIII tubulin-positive cells was conducted at 2 DIV analyzing the following three parameters that describe dendritic organization: total dendritic length, number of primary dendrites arising from the cell body, and number of branch points. Incubation of cultured neurons with either KN62 or LY294002 significantly reduced the total length of dentrites (ANOVA: $F = 24.75$, $p < 0.001$; NK t test, $p < 0.05$; KN62 and LY294002 vs vehicle, PD98059, and Rp-cAMP) (Fig. 6*L*), the number of primary dendrites (ANOVA: $F = 21.91$, $p < 0.001$; NK t test, $p < 0.05$; KN62 and LY294002 vs vehicle, PD98059, and Rp-cAMP) (Fig. 6*M*), and the number of branch points (ANOVA: $F = 24.75$, $p < 0.001$; NK t test, $p < 0.05$; KN62 and LY294002 vs vehicle and Rp-cAMP) (Fig. 6*N*) relative to control. The morphology of treated cells at 2 DIV as well as the percentage of CREB phosphorylation are reminiscent of those of control cells at 1 DIV (Fig. 6*B*,*G*,*H*), suggesting that KN62 and LY294002 treatments impair cell differentiation through inhibition of CREB function. In contrast, incubation of cultured neurons with either PD98059 or Rp-cAMP did not significantly influence the morphological dif-

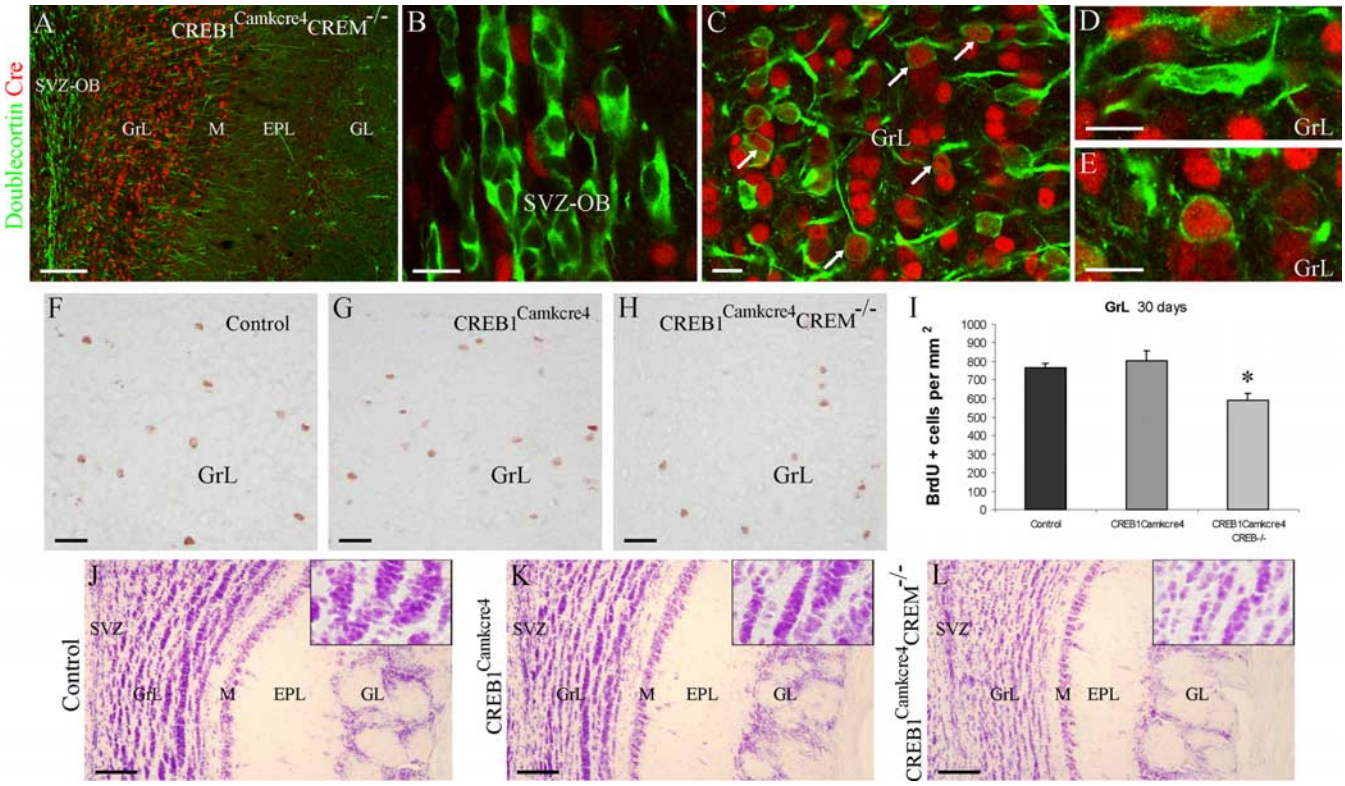

Figure 7. Reduced survival of newly generated cells in the OB of CREB1^{Camkcre4}CREM$^{-/-}$ double mutants. ***A–E***, Camkcre4 transgenics show high Cre recombinase expression in the OB GrL (***A***, ***C***). Few Cre-positive/doublecortin-negative cells are scattered within the SVZ-OB (***B***). Cre expression occurs in some polygonal- or round-shaped doublecortin-positive neuroblasts in the OB-GrL (***C***, arrows; ***E***). Bipolar radially migrating neuroblasts are Cre negative (***D***). BrdU+ nuclei in the OB GrL of control (***F***), CREB1^{Camkcre4} mutants (***G***), and CREB1^{Camkcre4}CREM$^{-/-}$ double mutants (***H***) 30 d after injection. A significant decrease in the density of newly generated cells is detected in the GrL of double mutants (***H***, ***I***). Cresyl violet staining in 5-month-old double mutants shows a reduced GrL cell density (***L***) compared with control (***J***) and single mutant (***K***) mice. The asterisk indicates a significant difference from control and single mutant mice. M, Mitral cell layer. Error bars indicate SEM. Scale bars: ***A***, ***J–L***, 100 μm; ***B–E***, 10 μm; ***F–H***, 20 μm.

ferentiation of newly generated neurons (Fig. 6*L–N*), suggesting that these two signaling pathways are not implicated in the early maturation steps of SVZ neuroblasts.

CaM kinases and PI3 kinase are implicated in complex signaling transduction pathways that do not exclusively converge on CREB. Thus, to directly interfere with the CREB-mediated regulation of transcription, we transfected cultured SVZ cells with an expression vector containing a dominant-negative form of CREB (A-CREB; kindly provided by Dr. C. Vinson) that heterodimerizes selectively with endogenous CREB and inhibits its DNA binding activity (Ahn et al., 1998). To directly visualize the occurrence of transfection of living primary neurons, we constructed a pEGFP-C3-A-CREB expression vector. Cells transfected with the pEGFP-C3 empty vector served as a control. When cells were transfected at 0 DIV, GFP-positive cells were detected by 1 DIV, indicating expression of GFP-A-CREB fusion protein. Cells were fixed at 2 DIV and processed for βIII tubulin immunocytochemistry and for GFP immunocytochemistry, to better visualize processes of transfected cells (Fig. 6***O–R***). The extent of morphological differentiation of βIII tubulin/GFP colabeled neurons was determined. pEGFP-C3-A-CREB transfection strongly decreased the percentage of cells that extend dendritic processes (*t* test; $p < 0.01$) (Fig. 6*S*). However, medium values of the total dendritic length, number of primary dendrites, and number of branch points were not significantly changed by pEGFP-C3-A-CREB transfection (dendritic length: control, 51.1 $\pm$ 7.7 μm; A-CREB, 39.6 $\pm$ 4.6 μm: *t* test, $p = 0.24$; number of primary dendrites: control, 1.6 $\pm$ 0.2 μm; A-CREB, 1.2 $\pm$ 0.08 μm; *t* test, $p = 0.1$; number of branches: control, 0.5 $\pm$ 0.06 μm; A-CREB, 0.35 $\pm$ 0.04 μm; *t* test, $p = 0.08$). These results demonstrate that GFP-A-CREB interferes with morphological differentiation of cultured SVZ neuronal precursors and suggest that CREB is particularly implicated in the regulation of the early phase of this process.

Survival of SVZ-derived newly generated cells is impaired in adult mice lacking both CREB and CREM

To investigate the effects of the *in vivo* loss of CREB function on OB neurogenesis, we analyzed the SVZ/OB system of transgenic mice (CREB1^{Camkcre4} mutants) in which CREB was postnatally disrupted using the Cre/loxP system (Mantamadiotis et al., 2002). We also analyzed neurogenesis in mice postnatally lacking CREB in a null CREM genetic background (CREB1^{Camkcre4}CREM$^{-/-}$ double mutants), because in CREB mutant mice, the related protein CREM is upregulated in many organs (Hummler et al., 1994) and can functionally compensate for CREB in the brain (Mantamadiotis et al., 2002). In these two strains of mice, Cre recombinase is robustly expressed in the postnatal forebrain under the control of the promoter of the calcium/CaM-dependent protein kinase II α gene (Mantamadiotis et al., 2002).

As a first step, to analyze whether recombination occurs in newly generated cells, we studied the expression of Cre recombinase in the SVZ/OB system. High levels of Cre immunoreactivity were detected in the GrL of the OB and in granule-like cells located in the mitral cell layer (Fig. 7*A*, *C*). Cre expression was low in the other OB layers; it was localized in scattered cells (Fig. 7*A*). In the OB GrL, double immunostaining for Cre and doublecortin showed a certain number of colabeled cells with polygonal or

rounded cell bodies (Fig. 7*C*,*E*). Here, doublecortin-positive cells with a bipolar morphology, reminiscent of migrating neuroblasts, were Cre immunonegative (Fig. 7*D*). Accordingly, the few Cre-positive cells located in the SVZ did not colocalize with the neuroblast marker doublecortin (Fig. 7*B*). These results indicate that Cre recombinase is expressed in neuroblasts only in the postmigratory phase once the cells have reached the GrL in the OB and have started their morphological differentiation.

The finding that Cre-mediated recombination in newly generated cells occurs starting from this phase prompted us to concentrate our analysis on the possible influence of CREB loss on the survival of newborn cells. To this purpose, newly generated cells were labeled by BrdU treatments on 3-month-old mice and quantified 30 d later in the OB GrL of controls, CREB1^{Camkcre4} single mutants, and CREB1^{Camkcre4}CREM$^{-/-}$ double mutants (Fig. 7***F–H***). The density of BrdU-labeled cells surviving in the GrL of double mutants was significantly decreased compared with that of control mice and single mutants (25% decrease; ANOVA: $F = 8.94$, $p < 0.01$; NK *t* test, $p < 0.05$; double mutants vs control mice and single mutants) (Fig. 7*I*). In agreement with the analysis of the distribution of BrdU-positive cells, an increased density of activated caspase-3-positive cells was found in the GrL of double-mutant mice (280% increase; control, 1.42 ± 0.19 cells/mm^2; single mutants, 1.52 ± 0.42 cells/mm^2; double mutants, 4.11 ± 0.78 cells/mm^2; ANOVA: $F = 5.55$, $p < 0.05$; NK *t* test, $p < 0.05$; double mutants vs control mice and single mutants). Thus, in the absence of CREM, loss of CREB impairs survival of newly generated neurons in the OB GrL. The involvement of CREB and CREM in granule cells survival is also supported by analysis of the OB morphology, visualized by cresyl violet staining at different ages. Indeed, a reduction in the thickness of the GrL and EPL was observed in double-mutant mice aged 5–7 months (Fig. 7***J–L***). This is probably attributable to a progressive reduction in GrL cell density (Fig. 7***J–L***, insets) that is not observed in younger mice (3–4 months old). Interestingly, no defects were observed in the OB of CREB1^{Camkcre4} single mutants (Fig. 7*K*) or CREM$^{-/-}$ single mutants (data not shown) at any stage analyzed, indicating that the loss of only CREM or only CREB does not influence cell survival. These results demonstrate that the CREB family of transcription factors is involved in the regulation of granule cell survival, including SVZ-derived newborn neurons, and suggest that CREM can functionally compensate for CREB in the regulation of adult OB neurogenesis.

Disruption of functional connections from the olfactory epithelium to the OB reduces neurogenesis and CREB phosphorylation in newly generated cells

Several studies indicate that the olfactory input can regulate neurogenesis in the OB. In particular, it has been demonstrated that recruitment and survival of SVZ neuroblasts in the OB are in part dependent on incoming activity from the olfactory epithelium both during early postnatal development and in adulthood (Frazier-Cierpial and Brunjes, 1989; Cummings and Brunjes, 1997; Cummings et al., 1997; Petreanu and Alvarez-Buylla, 2002; Rochefort et al., 2002; Saghatelyan et al., 2004). Deprivation of the olfactory input by various experimental approaches has been shown to impair radial migration/survival of newly generated cells and to increase cell death (Frazier-Cierpial and Brunjes, 1989; Cummings and Brunjes, 1997; Petreanu and Alvarez-Buylla, 2002; Saghatelyan et al., 2004), but the molecular mechanism involved is not known. To investigate a possible relationship between olfactory peripheral afferents, the supply of newborn neurons to the OB, and CREB activation in neuroblasts, we analyzed neurogenesis and CREB phosphorylation in an experimental model of sensory deprivation. In the present study, intranasal irrigation with zinc sulfate was performed to disrupt connections from the olfactory epithelium to the OB (McBride et al., 2003). OMP immunohistochemistry was used to assess anatomical connectivity between the olfactory epithelium and bulb after zinc sulfate treatment (Cummings et al., 2000). Only the animals showing a sharp reduction in the olfactory nerve and GLs (Fig. 8*A*,*B*) were considered for the study. To assess the effect of our experimental protocol on neurogenesis, newly generated cells were labeled by BrdU treatments and quantified 10, 15, and 45 d later in the OB of control and treated mice (Fig. 8). The density of BrdU-labeled cells in the SVZ-OB of treated mice was strongly increased 10 d after BrdU injection compared with that of control mice (291% increase; *t* test; $p < 0.05$) (Fig. 8*C*,*D*,*G*). A highly significant difference was still present at 15 d survival (206% increase; *t* test; $p < 0.02$) (Fig. 8*G*). These results indicate an accumulation of newly generated cells in the SVZ-OB. The analysis of the distribution of BrdU-positive cells in the OB GrL showed that both 10 and 15 d after BrdU injection, the density of labeled cells in the superficial GrL, but not that in the deep GrL, was lower in treated mice compared with controls (Fig. 8*C*,*D*,*H*) (*t* test; $p < 0.02$ at 10 d and $p < 0.05$ at 15 d; saline vs zinc sulfate in the superficial GrL). Moreover, the density of BrdU-positive cells after 45 d survival was reduced in the entire GrL of zinc sulfate-treated mice compared with control mice (32% decrease; *t* test; $p < 0.01$) (Fig. 8*E*,*F*,*I*). These results suggest that chemical deafferentation of the bulb induces a reduction and/or a delay in neuroblast radial migration out of the SVZ and impairs survival of newly generated cells in the GrL. In support of this hypothesis, 2 weeks after intranasal irrigation, a high density of cells positive for activated caspase-3, which has been shown to be implicated in programmed cell death (Srinivasan et al., 1998), was found in the SVZ-OB and OB GrL of zinc sulfate-treated mice (Fig. 8*J–L*) (*t* test; $p < 0.002$ in the SVZ-OB and $p < 0.02$ in the GrL; control vs zinc sulfate-treated mice). Approximately 20–30% of these cells were also labeled for doublecortin (Fig. 8*J*,*K*), supporting the hypothesis that after OB chemical deafferentation, a portion of newly generated elements fail to differentiate and eventually die. We thus analyzed whether the deafferentation protocol affected also CREB expression and/or its phosphorylation in the SVZ/OB system. Although no differences of CREB expression were observed between control and treated animals (Fig. 9*A*,*B*), the peripheral deafferentation strongly modified the pattern of CREB phosphorylation in the OB (Fig. 9*C–F*). Here, in contrast to the increase registered for BrdU-positive cells in the SVZ, the number of pCREB-immunopositive cells was sharply reduced. Quantification of CREB phosphorylation in doublecortin-positive neuroblasts 9, 14, and 44 d after zinc sulfate treatment confirmed that the percentage of double-positive neuroblasts was dramatically decreased in the SVZ-OB after treatment (Fig. 9*G*) (ANOVA; $F = 8.80$; $p < 0.001$). The decrease was highly significant at 15 and 44 d (Fig. 9*G*) (NK *t* test; $p < 0.05$; saline vs zinc), suggesting that functional connections from the olfactory epithelium are required to initiate CREB phosphorylation in neuroblasts reaching the OB, before they start to migrate radially out of the SVZ. Unlike the SVZ, no changes in the percentage of doublecortin-positive neuroblasts labeled for pCREB were observed in the GrL and GL of the OB at any time after intranasal irrigation (Fig. 9*H*,*I*). Thus, the reduced number of newly generated cells that move radially out of the SVZ after chemical deafferentation of the OB are pCREB positive. pCREB immunoreactivity was increased in numerous mature elements in the GrL (Fig. 9*D*), mitral layer, and GL of treated mice (data not shown). Together, these data show a correlation between

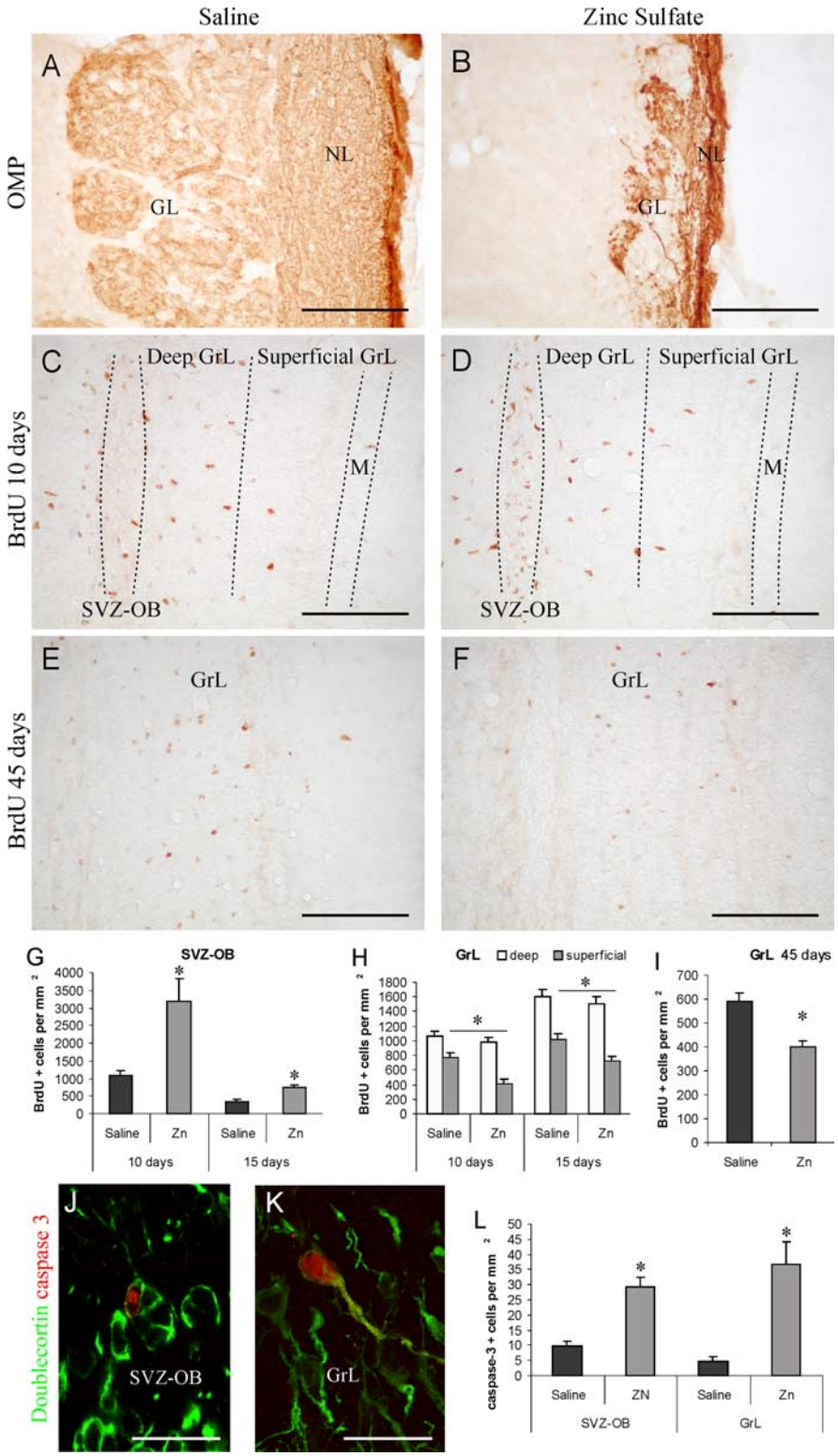

Figure 8. Chemical lesions of the olfactory epithelium reduce neurogenesis in the olfactory bulb. ***A***, ***B***, Zinc sulfate intranasal irrigation produces disruption of functional connections from the olfactory epithelium to the OB. OMP-positive axons of olfactory receptor neurons projecting to the OB are dramatically reduced in the OB NL and GL of zinc sulfate-treated mice (***B***) compared with controls (***A***). ***C***, ***D***, BrdU immunoreactivity in control (***C***) and zinc sulfate-treated mice (***D***) 10 d after BrdU injection. Note the higher density of BrdU+ nuclei in the SVZ-OB of treated mice (***D***). Conversely, a reduced density of BrdU+ nuclei is seen within the superficial GrL of treated mice (***D***). ***E***, ***F***, BrdU immunoreactivity in control (***E***) and zinc sulfate-treated mice (***F***) 45 d after BrdU injection. Note the reduced density of BrdU+ nuclei in the SVZ-OB of treated mice. ***G***, Quantification of BrdU+ nuclei in the SVZ-OB of control and zinc sulfate-treated mice indicates a significant increase in the density of newly generated cells in the SVZ-OB of treated mice both 10 and 15 d after BrdU injection. ***H***, Quantification of BrdU+ nuclei in the OB GrL of control and zinc sulfate-treated mice 10 and 15 d after BrdU injection. A significant decrease in the density of newly generated cells is detected in the superficial GrL of treated mice. ***I***, Significant reduction in the density of BrdU-labeled cells surviving for 45 d in the GrL of zinc sulfate-treated mice. ***J***, ***K***, Doublecortin/activated caspase-3 double-labeled cells in the OB of zinc sulfate-treated mice 2 weeks after intranasal irrigation. Note a double-labeled cell within a chain of tangentially migrating cells in the SVZ-OB (***J***) and a radially oriented double-labeled cell in the OB GrL (***K***). ***L***, Significant increase in the density of activated caspase-3-immunoreactive cells in the SVZ-OB and OB GrL of zinc sulfate-treated mice 2 weeks after irrigation. The asterisk indicates a significant difference from saline controls. M, Mitral cell layer; NL, olfactory nerve layer; Zn, zinc sulfate. Error bars indicate SEM. Scale bars: ***A–D***, 100 μm; ***H***, ***I***, 20 μm.

the peripheral input, cell migration and survival, and levels of CREB phosphorylation.

Discussion

In this study, we demonstrate the involvement of the transcription factor CREB in the regulation of differentiation and survival of neuronal precursors of the adult SVZ. Our *in vivo* analyses indicate that although CREB is expressed in the SVZ/OB system from dividing precursors to mature OB interneurons, its active/phosphorylated form is transient and associated with specific stages of the neurogenic process (Fig. 10*A*). Strong CREB phosphorylation occurs during the last part of the SVZ neuroblast migration and persists in the early stages of differentiation. To precisely correlate CREB activation and the maturation stages of newly generated cells, we adopted a cell transplant approach using EGFP transgenic mice as donors. This method led us to establish that CREB phosphorylation is still present during dendrite elongation and arborization, up to spine formation. Once attained a mature morphology, the majority of newly generated cells downregulate pCREB. Transient CREB phosphorylation has been demonstrated previously in neuroblasts of the adult dentate gyrus (Nakagawa et al., 2002b), where this transcription factor regulates several steps of the neurogenic process, including proliferation, differentiation, and survival (Nakagawa et al., 2002a,b; Fujioka et al., 2004). In the present work, the pattern of CREB phosphorylation suggests an involvement of this transcription factor in differentiation rather than proliferation, because it was mostly absent in dividing cells of the SVZ. The implication of CREB in the maturation of SVZ neuronal precursors was confirmed *in vitro* using primary cultures. First, we showed that the *in vivo* pattern of CREB phopshorylation was mimicked during neuronal differentiation in our *in*

vitro model. Second, inhibitors of CaM and PI3 protein kinases significantly reduced CREB phosporylation and morphological differentiation (dendritic branching, length, and number) of SVZ newborn neurons, whereas inhibitors of MAP- and cAMP-dependent protein kinases did not affect CREB phosphorylation and differentiation of these cells. Notably, it has been demonstrated previously that inhibition of the cAMP signaling reduces CREB phosphorylation in newly generated cells of the hippocampus (Fujioka et al., 2004), suggesting that different pathways are implicated in CREB activation in the two adult neurogenic areas. Third, transfection of a dominant-negative form of CREB, which prevents its DNA-binding activity, impaired maturation of SVZ neuroblasts. The differentiation-promoting action of CREB has been demonstrated previously *in vitro* and *in vivo*. Pharmacological activation of the cAMP–CREB cascade increases differentiation of adult-derived hippocampal progenitor cells (Palmer et al., 1997; Fujioka et al., 2004), whereas blocking CREB function attenuates outgrowth of cortical neuron dendrites (Redmond et al., 2002) and decreases the number of branches and length of processes in young granule cells of the dentate gyrus (Fujioka et al., 2004). Moreover, experimental evidence indicates that CREB activation may occur directly in developing dendrites (Crino et al., 1998) and is important for the formation of new spines (Murphy and Segal, 1997; Bender et al., 2001). Together with these studies, our data support a central role for CREB in neuronal differentiation.

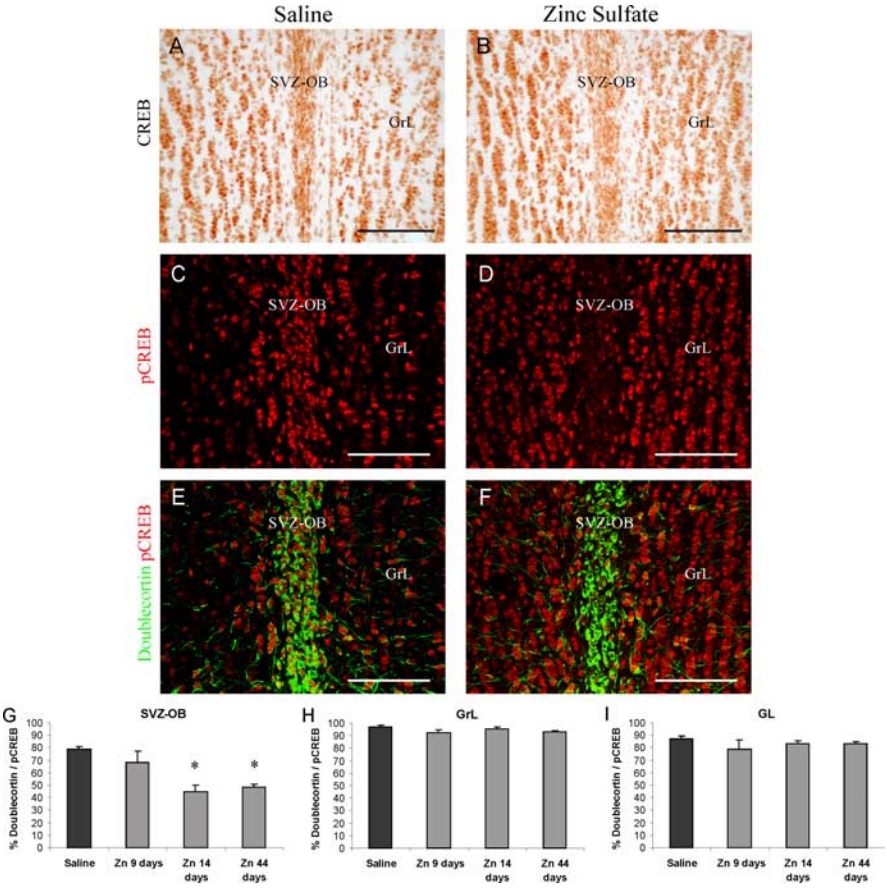

Figure 9. Chemical lesions of the olfactory epithelium reduce pCREB immunoreactivity in newly generated cells. ***A***, ***B***, CREB immunoreactivity in control (***A***) and zinc sulfate-treated (***B***) mice. Note that CREB immunoreactivity is not reduced after an olfactory lesion. ***C–F***, pCREB immunoreactivity is strongly reduced in the SVZ-OB of zinc sulfate-treated mice. In control mice, strong pCREB immunoreactivity is found in doublecortin-positive neuroblasts within the SVZ-OB (***C***, ***E***). In contrast, an olfactory lesion strongly reduces pCREB in tangentially migrating neuroblasts (***D***, ***F***). An increase in pCREB immunoreactivity is observed in the OB GrL after an olfactory lesion (***D***). ***G–I***, Quantification of doublecortin-positive neuroblasts expressing pCREB in the SVZ-OB (***G***), OB GrL (***H***), and GL (***I***). Data are presented as the percentage of doublecortin+ cells. Two weeks and 44 d after zinc sulfate treatment, pCREB immunoreactivity is strongly reduced in tangentially migrating neuroblasts within the SVZ-OB (***G***) but not in radially migrating/differentiating neuroblasts within the GrL (***H***) and GL (***I***). The asterisk indicates a significant difference from saline controls. Images ***A–H*** are from mice killed 2 weeks after intranasal irrigation. Error bars indicate SEM. Scale bars, 100 μm. Zn, Zinc sulfate.

The specific genes responsible for the action of CREB on the maturation of SVZ newborn neurons are not yet characterized. Neuronal differentiation of SVZ neuroblasts initiates early during radial migration and passes through a unique sequence of events involving the expression of neurotransmitter receptors and rate-limiting enzymes in neurotransmitters biosynthesis (Baker et al., 2001; Carleton et al., 2003). For instance, the transcription of the tyrosine hydroxylase gene occurs in SVZ newly generated cells before they attain their final periglomerular position (Baker et al., 2001; Saino-Saito et al., 2004). Interestingly, it has been shown that CREB participates in the Cre DNA–protein complex of the tyrosine hydroxylase promoter in the mouse OB (Liu et al., 1999). These results are consistent with a role for CREB in regulating the transcription of genes involved in the differentiation of SVZ neuroblasts.

In addition to differentiation, our *in vivo* data also support a role for CREB in the survival of SVZ neuronal precursors. In fact, BrdU time course analysis and morphological studies on EGFP engrafted cells demonstrated that the majority of newly generated cells downregulate CREB phosphorylation after 1 month of survival into the OB. This time point corresponds to the end of a selection-critical period, after which the number of newly generated cells remains relatively constant (Petreanu and Alvarez-Buylla, 2002; Carleton et al., 2003). We can thus infer that CREB-mediated transcriptional mechanisms may also be involved in controlling long-term functional integration. This view is also supported by peripheral afferent denervation experiments that determine reduced survival of the newly generated cells in the OB and a parallel downregulation of CREB phosphorylation in SVZ progenitors (Fig. 10*B*). We directly tested the possibility that CREB influences survival of newly generated cells by using transgenic mice lacking CREB in the postnatal forebrain through the Cre/loxP system (Mantamadiotis et al., 2002). We showed that in these mice, disruption of CREB in neuroblasts occurs after their radial migration has been completed, just before the selection-critical period. Loss of CREB during this phase, in a null CREM genetic background, significantly reduces the survival of newborn neurons (Fig. 10*C*). No effects were found in CREB single-mutant mice. These results are in agreement with previous studies showing that CREB and CREM transcription factors cooperate and that CREM upregulation can functionally com-

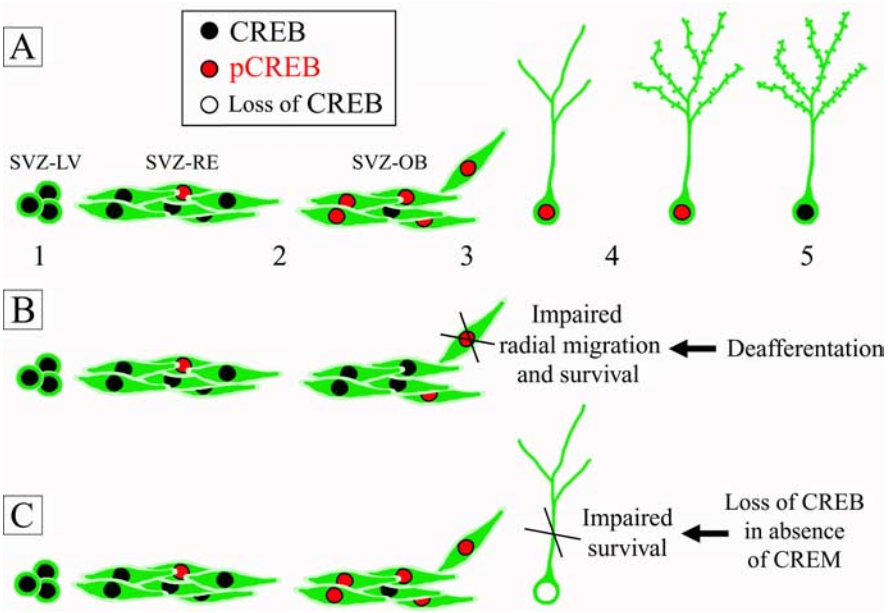

Figure 10. Schematic drawing of CREB expression/phosphorylation in SVZ newly generated cells throughout neurogenesis in normal conditions (***A***), after ZnSO4 deafferentation (***B***), and in CREB1^{Camkcre4}CREM$^{-/-}$ double mutants (***C***). ***A***, Although CREB is expressed by newly generated cells from cell genesis (1) to integration into the OB (5), CREB phosphorylation occurs at the shift from tangential (2) to radial migration (3), persists during cell differentiation (4), and is downregulated after attainment of a fully mature morphology (5). ***B***, Olfactory peripheral deafferentation results in downregulation of CREB phosphorylation in SVZ neuroblasts, the radial migration and survival of which appear heavily impaired. ***C***, In CREB1^{Camkcre4}CREM$^{-/-}$ double mutants, Cre-mediated recombination in neuroblasts occurs in the early postmigratory phase. Loss of CREB at this stage impairs survival of newly generated cells.

pensate for CREB in the brain (Hummler et al., 1994; Mantamadiotis et al., 2002). These data demonstrate that CREB family members are crucial in OB granule cell survival and suggest that functions of CREB and CREM are partially overlapping.

According to the prevailing view, phosphorylation of CREB represents a convergence point downstream of a vast array of extracellular stimuli, such as growth factors and neurotransmitters (Lonze and Ginty, 2002). In the OB, several studies indicated an activity-dependent modulation of CREB phosphorylation in different cell types. Indeed, CREB is activated in mitral cells by odor-preference learning (McLean et al., 1999), and a trend to an increase in CREB phosporylation in external OB layers has been observed after unilateral naris closure (Liu et al., 1999). In this study, we demonstrate that CREB phosphorylation is upregulated in rostrally migrating neuroblasts when they reach the OB but sharply decreases after olfactory peripheral afferent denervation (Fig. 10*B*). These results suggest the existence of molecular factors expressed in the OB that induce CREB phosphorylation in SVZ newly generated cells. We can thus hypothesize that disruption of functional connections from the olfactory epithelium determines changes in the OB molecular environment that in turn reduce CREB phosphorylation in newly generated cells (Fig. 10*B*). Interestingly, several studies have demonstrated that the olfactory input modulates the expression of molecules, such as tenascin-R (Saghatelyan et al., 2004) and BDNF (McLean et al., 2001), that promote migration, differentiation, and survival of neuronal precursors arising from the SVZ (Kirschenbaum and Goldman, 1995; Goldman et al., 1997; Gascon et al., 2005).

Although an involvement of the transcription factor CREB in cell differentiation and survival is not surprising, as demonstrated previously in different neuronal types (Murphy and Segal, 1997; Crino et al., 1998; Bonni et al., 1999; Riccio et al., 1999; Walton et al., 1999; Monti et al., 2002; Redmond et al., 2002; Shalizi et al., 2003; Fujioka et al., 2004), its putative role in cell migration is puzzling. Nevertheless, it is noteworthy that peripheral afferent denervation of the OB also determines a sharp reduction in CREB phosphorylation in tangentially migrating neuroblasts, accumulation of newly generated cells in the SVZ-OB, and consequent reduced radial migration, whereas radially migrating and differentiating neuroblasts are pCREB immunoreactive. These data suggest that CREB phosphorylation is crucial for the progression through these processes. CREB might allow neuroblasts to move out of the SVZ by inducing the transcription of genes involved in radial migration. It has been hypothesized that NMDA receptors, which modulate radial neuronal migration in the developing brain (Komuro and Rakic, 1993, 1998), are also involved in radial migration within the adult OB (Saghatelyan et al., 2004). Indeed, radial migration in the OB correlates with the appearance of NMDA receptor-mediated currents in newly generated cells (Carleton et al., 2003). Notably, transcription of NMDA receptor subunit 1, required for functional receptor formation, is regulated in cortical neurons by the cAMP signaling pathway, most likely through CREB activation by signal-dependent phosphorylation (Lau et al., 2004). Additional studies will be required to ascertain an involvement of CREB-mediated transcription in the regulation of neuroblasts migration.

These overall results and considerations provide evidence that CREB activation has a functional implication in multiple aspects of adult OB neurogenesis.

References

Ahn S, Olive M, Aggarwal S, Krylov D, Ginty DD, Vinson C (1998) A dominant-negative inhibitor of CREB reveals that it is a general mediator of stimulus-dependent transcription of c-fos. Mol Cell Biol 18:967–977.

Altman J (1969) Autoradiographic and histological studies of postnatal neurogenesis. IV. Cell proliferation and migration in the anterior forebrain, with special reference to persisting neurogenesis in the olfactory bulb. J Comp Neurol 137:433–457.

Altman J, Das GD (1965) Autoradiographic and histological evidence of postnatal hippocampal neurogenesis in rats. J Comp Neurol 124:319–335.

Alvarez-Buylla A, Garcia-Verdugo JM (2002) Neurogenesis in adult subventricular zone. J Neurosci 22:629–634.

Baker H, Liu N, Chun HS, Saino S, Berlin R, Volpe B, Son JH (2001) Phenotypic differentiation during migration of dopaminergic progenitor cells to the olfactory bulb. J Neurosci 21:8505–8513.

Bender RA, Lauterborn JC, Gall CM, Cariaga W, Baram TZ (2001) Enhanced CREB phosphorylation in immature dentate gyrus granule cells precedes neurotrophin expression and indicates a specific role of CREB in granule cell differentiation. Eur J Neurosci 13:679–686.

Bonni A, Brunet A, West AE, Datta SR, Takasu MA, Greenberg ME (1999) Cell survival promoted by the Ras-MAPK signaling pathway by transcription-dependent and -independent mechanisms. Science 286:1358–1362.

Brown JP, Couillard-Despres S, Cooper-Kuhn CM, Winkler J, Aigner L, Kuhn HG (2003) Transient expression of doublecortin during adult neurogenesis. J Comp Neurol 467:1–10.

Cameron HA, Woolley CS, McEwen BS, Gould E (1993) Differentiation of newly born neurons and glia in the dentate gyrus of the adult rat. Neuroscience 56:337–344.

Canon E, Cosgaya JM, Scsucova S, Aranda A (2004) Rapid effects of retinoic acid on CREB and ERK phosphorylation in neuronal cells. Mol Biol Cell 15:5583–5592.

Carleton A, Petreanu LT, Lansford R, Alvarez-Buylla A, Lledo PM (2003) Becoming a new neuron in the adult olfactory bulb. Nat Neurosci 6:507–518.

Carletti B, Grimaldi P, Magrassi L, Rossi F (2002) Specification of cerebellar progenitors after heterotopic-heterochronic transplantation to the embryonic CNS *in vivo* and *in vitro*. J Neurosci 22:7132–7146.

Crino P, Khodakhah K, Becker K, Ginsberg S, Hemby S, Eberwine J (1998) Presence and phosphorylation of transcription factors in developing dendrites. Proc Natl Acad Sci USA 95:2313–2318.

Cummings DM, Brunjes PC (1997) The effects of variable periods of functional deprivation on olfactory bulb development in rats. Exp Neurol 148:360–366.

Cummings DM, Henning HE, Brunjes PC (1997) Olfactory bulb recovery after early sensory deprivation. J Neurosci 17:7433–7440.

Cummings DM, Emge DK, Small SL, Margolis FL (2000) Pattern of olfactory bulb innervation returns after recovery from reversible peripheral deafferentation. J Comp Neurol 421:362–373.

De Marchis S, Fasolo A, Shipley M, Puche A (2001) Unique neuronal tracers show migration and differentiation of SVZ progenitors in organotypic slices. J Neurobiol 49:326–338.

De Marchis S, Temoney S, Erdelyi F, Bovetti S, Bovolin P, Szabo G, Puche AC (2004) GABAergic phenotypic differentiation of a subpopulation of subventricular derived migrating progenitors. Eur J Neurosci 20:1307–1317.

Frazier-Cierpial L, Brunjes PC (1989) Early postnatal cellular proliferation and survival in the olfactory bulb and rostral migratory stream of normal and unilaterally odor-deprived rats. J Comp Neurol 289:481–492.

Fujioka T, Fujioka A, Duman RS (2004) Activation of cAMP signaling facilitates the morphological maturation of newborn neurons in adult hippocampus. J Neurosci 24:319–328.

Gascon E, Vutskits L, Zhang H, Barral-Moran MJ, Kiss PJ, Mas C, Kiss JZ (2005) Sequential activation of p75 and TrkB is involved in dendritic development of subventricular zone-derived neuronal progenitors in vitro. Eur J Neurosci 21:69–80.

Goldman SA, Kirschenbaum B, Harrison-Restelli C, Thaler HT (1997) Neuronal precursors of the adult rat subependymal zone persist into senescence, with no decline in spatial extent or response to BDNF. J Neurobiol 32:554–566.

Hummler E, Cole TJ, Blendy JA, Ganss R, Aguzzi A, Schmid W, Beermann F, Schutz G (1994) Targeted mutation of the CREB gene: compensation within the CREB/ATF family of transcription factors. Proc Natl Acad Sci USA 91:5647–5651.

Jankovski A, Sotelo C (1996) Subventricular zone-olfactory bulb migratory pathway in the adult mouse: cellular composition and specificity as determined by heterochronic and heterotopic transplantation. J Comp Neurol 371:376–396.

Kirschenbaum B, Goldman SA (1995) Brain-derived neurotrophic factor promotes the survival of neurons arising from the adult rat forebrain subependymal zone. Proc Natl Acad Sci USA 92:210–214.

Komuro H, Rakic P (1993) Modulation of neuronal migration by NMDA receptors. Science 260:95–97.

Komuro H, Rakic P (1998) Orchestration of neuronal migration by activity of ion channels, neurotransmitter receptors, and intracellular Ca^{2+} fluctuations. J Neurobiol 37:110–130.

Lau GC, Saha S, Faris R, Russek SJ (2004) Up-regulation of NMDAR1 subunit gene expression in cortical neurons via a PKA-dependent pathway. J Neurochem 88:564–575.

Liu N, Cigola E, Tinti C, Jin BK, Conti B, Volpe BT, Baker H (1999) Unique regulation of immediate early gene and tyrosine hydroxylase expression in the odor-deprived mouse olfactory bulb. J Biol Chem 274:3042–3047.

Lois C, Alvarez-Buylla A (1994) Long-distance neuronal migration in the adult mammalian brain. Science 264:1145–1148.

Lonze BE, Ginty DD (2002) Function and regulation of CREB family transcription factors in the nervous system. Neuron 35:605–623.

Luskin MB (1993) Restricted proliferation and migration of postnatally generated neurons derived from the forebrain subventricular zone. Neuron 11:173–189.

Mantamadiotis T, Lemberger T, Bleckmann SC, Kern H, Kretz O, Martin Villalba A, Tronche F, Kellendonk C, Gau D, Kapfhammer J, Otto C, Schmid W, Schutz G (2002) Disruption of CREB function in brain leads to neurodegeneration. Nat Genet 31:47–54.

McBride K, Slotnick B, Margolis FL (2003) Does intranasal application of zinc sulfate produce anosmia in the mouse? An olfactometric and anatomical study. Chem Senses 28:659–670.

McLean JH, Darby-King A, Bonnell WS (2001) Neonatal olfactory sensory deprivation decreases BDNF in the olfactory bulb of the rat. Brain Res Dev Brain Res 128:17–24.

Monti B, Marri L, Contestabile A (2002) NMDA receptor-dependent CREB activation in survival of cerebellar granule cells during in vivo and in vitro development. Eur J Neurosci 16:1490–1498.

Murphy DD, Segal M (1997) Morphological plasticity of dendritic spines in central neurons is mediated by activation of cAMP response element binding protein. Proc Natl Acad Sci USA 94:1482–1487.

Nakagawa S, Kim JE, Lee R, Malberg JE, Chen J, Steffen C, Zhang YJ, Nestler EJ, Duman RS (2002a) Regulation of neurogenesis in adult mouse hippocampus by cAMP and the cAMP response element-binding protein. J Neurosci 22:3673–3682.

Nakagawa S, Kim JE, Lee R, Chen J, Fujioka T, Malberg J, Tsuji S, Duman RS (2002b) Localization of phosphorylated cAMP response element-binding protein in immature neurons of adult hippocampus. J Neurosci 22:9868–9876.

Okabe M, Ikawa M, Kominami K, Nakanishi T, Nishimune Y (1997) "Green mice" as a source of ubiquitous green cells. FEBS Lett 407:313–319.

Palmer TD, Takahashi J, Gage FH (1997) The adult rat hippocampus contains primordial neural stem cells. Mol Cell Neurosci 8:389–404.

Peretto P, Merighi A, Fasolo A, Bonfanti L (1999) The subependymal layer in rodents: a site of structural plasticity and cell migration in the adult mammalian brain. Brain Res Bull 49:221–243.

Petreanu L, Alvarez-Buylla A (2002) Maturation and death of adult-born olfactory bulb granule neurons: role of olfaction. J Neurosci 22:6106–6113.

Petridis AK, El-Maarouf A, Rutishauser U (2004) Polysialic acid regulates cell contact-dependent neuronal differentiation of progenitor cells from the subventricular zone. Dev Dyn 230:675–684.

Redmond L, Kashani AH, Ghosh A (2002) Calcium regulation of dendritic growth via CaM kinase IV and CREB-mediated transcription. Neuron 34:999–1010.

Riccio A, Ahn S, Davenport CM, Blendy JA, Ginty DD (1999) Mediation by a CREB family transcription factor of NGF-dependent survival of sympathetic neurons. Science 286:2358–2361.

Rochefort C, Gheusi G, Vincent JD, Lledo PM (2002) Enriched odor exposure increases the number of newborn neurons in the adult olfactory bulb and improves odor memory. J Neurosci 22:2679–2689.

Rodgers EE, Theibert AB (2002) Functions of PI 3-kinase in development of the nervous system. Int J Dev Neurosci 20:187–197.

Saghatelyan A, de Chevigny A, Schachner M, Lledo PM (2004) Tenascin-R mediates activity-dependent recruitment of neuroblasts in the adult mouse forebrain. Nat Neurosci 7:347–356.

Saino-Saito S, Sasaki H, Volpe BT, Kobayashi K, Berlin R, Baker H (2004) Differentiation of the dopaminergic phenotype in the olfactory system of neonatal and adult mice. J Comp Neurol 479:389–398.

Sambrook J, Fritsch EF, Maniatis T (1999) Molecular cloning: a laboratory manual, Ed 2. Cold Spring Harbor, NY: Cold Spring Harbor Laboratory.

Shalizi A, Lehtinen M, Gaudilliere B, Donovan N, Han J, Konishi Y, Bonni A (2003) Characterization of a neurotrophin signaling mechanism that mediates neuron survival in a temporally specific pattern. J Neurosci 23:7326–7336.

Shingo T, Gregg C, Enwere E, Fujikawa H, Hassam R, Geary C, Cross JC, Weiss S (2003) Pregnancy-stimulated neurogenesis in the adult female forebrain mediated by prolactin. Science 299:117–120.

Srinivasan A, Roth KA, Sayers RO, Shindler KS, Wong AM, Fritz LC, Tomaselli KJ (1998) In situ immunodetection of activated caspase-3 in apoptotic neurons in the developing nervous system. Cell Death Differ 5:1004–1016.

Walton M, Woodgate AM, Muravlev A, Xu R, During MJ, Dragunow M (1999) CREB phosphorylation promotes nerve cell survival. J Neurochem 73:1836–1842.

Winner B, Cooper-Kuhn CM, Aigner R, Winkler J, Kuhn HG (2002) Long-term survival and cell death of newly generated neurons in the adult rat olfactory bulb. Eur J Neurosci 16:1681–1689.